

Transverse Momentum Dependence of the Landau-Pomeranchuk-Migdal Effect

Urs Achim Wiedemann and Miklos Gyulassy

Physics Department, Columbia University, New York, NY 10027, USA

(April 16, 2018)

We study the transverse momentum dependence of the Landau-Pomeranchuk-Migdal effect in QED, starting from the high energy expansion of the solution of the Dirac equation in the presence of an external field. The angular integrated energy loss formula differs from an earlier expression of Zakharov by taking finite kinematical boundaries into account. In an expansion in powers of the opacity of the medium, we derive explicit expressions for the radiation cross section associated with $N = 1, 2$ and 3 scatterings. We verify the Bethe-Heitler and the factorization limit, and we calculate corrections to the factorization limit proportional to the square of the target size. A closed form expression valid to arbitrary orders in the opacity is derived in the dipole approximation. The resulting radiation spectrum is non-analytic in the coupling constant which is traced back to the transverse momentum broadening of a hard parton undergoing multiple small angle Molière scattering. In extending the results to QCD, we test a previously used dipole prescription by comparing to direct pQCD results for $N = 1$ and 2. For $N = 1$, the QCD dipole prescription reproduces exactly the Bertsch-Gunion radiation spectrum. For $N = 2$, we find a sizeable correction which reduces to a multiplicative factor $17/8$ at large separation.

I. INTRODUCTION

In QED, the Landau-Pomeranchuk-Migdal (LPM) effect interpolates between the Bethe-Heitler and factorization limit for the radiation spectrum of a charged particle undergoing multiple, N say, scatterings in a medium. If the separation between scattering centers is very large, then the radiation off these centers reduces to a sum of radiation spectra for N small-angle scatterings - this is the Bethe-Heitler limit. In the opposite limit, when the scattering centers sit too close together to be resolved by the emitted photon, the observed radiation factorizes into a product of a single scattering Bethe-Heitler spectrum for momentum transfer $q = \sum_{i=1}^N q_i$ and the elastic cross section for the momentum transfer q accumulated over N small-angle scatterings.

As first noted by Landau and Pomeranchuk [1, 2], the relevant length scale for the interpolation between Bethe-Heitler and factorization limit is the coherence length (formation length) l_f , determined by the longitudinal momentum transfer q_l ,

$$l_f = 1/q_l. \quad (1.1)$$

This characterizes the longitudinal scale on which the radiated particle becomes distinguishable from its radiating parent. Scattering amplitudes for the radiation off different scattering centers interfere destructively if their separation is less than l_f : the *coherent* factorization limit is suppressed in the ultrarelativistic limit with respect to the *incoherent* Bethe-Heitler limit.

For a quantitative description of the LPM interference effect, the relative phases of the different contributions to the N -fold scattering amplitude matter. These depend on the transverse energies and thus require knowledge about the transverse motion of the radiating particle in the medium. Migdal [3] was the first to develop a dynamical description to this aim, employing a two-dimensional Fokker-Planck transport equation [3, 4] for the hard parton. In the limit of an infinite medium, his well-known result shows a characteristic $\propto \sqrt{\omega}$ low frequency suppression of $dN_\gamma/d\log\omega$ compared to the constant dependence in the Bethe-Heitler limit, i.e., the coherent factorization limit for $\omega \rightarrow 0$ vanishes. This is, however, only a very special feature of Migdal's limiting case, where the formation length goes to infinity for $\omega \rightarrow 0$, but never exceeds the (infinite) extension L of the medium. For a medium of finite size, the formation length does exceed the system size below some critical frequency ω_{cr} , and the Bethe-Heitler limit is finite. Migdal's $\sqrt{\omega}$ -dependence is hence not valid for $\omega < \omega_{cr}$. Moreover, additional effects become important for the radiation spectrum at lower frequencies [5]. Most notably, this is the transition radiation and the Ter-Mikaelian effect [6] of dielectric suppression.

The renewed interest in the LPM-effect has at least two reasons: On the one hand, forty years after discovering the theoretical principles [1, 3], the first precision measurements of the LPM-effect [7, 8] (and the Ter-Mikaelian effect [8, 9]) were made recently by the SLAC-146 collaboration. On the other hand, with the advent of a new generation of relativistic heavy ion colliders at RHIC and LHC, the understanding of the non-abelian analogue becomes important.

In the QED case, the experiment explored relatively thin targets with L/l_f on the order 0.1 to 10, in which the transition between Bethe-Heitler and factorization limit occurs. For a quantitative understanding, a realistic theory has to account for the finite extension of the target, the multiple elastic scatterings in the target, multiple photon emission, and possibly additional complications like radiation off structured targets.

There are at least three modern approaches, which can

account in principle for the LPM-effect in realistic targets. They implement the eikonal approximation for the radiating hard particle in different ways: i) Blankenbecler and Drell [10, 11] (see also Baier and Katkov [12, 13, 14]) started from the solution of the Klein-Gordon equation for the charged particle in the presence of an external field. The solution was approximated to order $1/E$ in a high energy expansion in which the eikonal path of the radiating particle is recovered. ii) Zakharov [15] proposed a light-cone path integral formulation which describes in a coordinate-space representation the transverse momentum kicks on the eikonal path, mimicking the elastic scatterings by an effective dipole cross section. Zakharov's work [16, 17] provides the most accurate description of the measured data so far. As we shall see in section II C, his starting point is closely related to a high energy expansion of the Dirac equation in the presence of an external potential. iii) A third approach is due to R. Baier et al. (BDMPS) [18], who started from the radiation amplitudes for N -fold scattering in the eikonal approximation. For QED, the consistency of their approach and the work of Blankenbecler and Drell can be checked diagrammatically [19]. A discussion of the LPM effect also exists for non-equilibrium conditions [20].

In the QCD case, high $p_t \leq 10$ GeV jets will be one of the new probes of the dense matter produced in relativistic heavy ion collisions. Deviations from factorized perturbative QCD due to final state rescattering are sensitive to the density and coupling in the plasma and will affect key observables like the high momentum tails of single particle spectra. The corresponding study of QCD radiative energy loss due to final state rescattering was initiated by Gyulassy and Wang [21, 22]. Recently, it has been extended most notably in a series of papers by BDMPS [23, 24, 25, 26] using equal time perturbation theory. Also, Zakharov has pointed out that his formalism can be adopted to QCD bremsstrahlung with a dipole prescription [15, 17], and the equivalence of Zakharov's formalism with the work of BDMPS was sketched [26].

All these calculations of the LPM-effect in QCD, however, are (1) limited to the cases of infinitely many or very few ($N < 3$) rescatterings of the parton, and (2) they mainly focus on the angular integrated energy loss $dE/dx dL$ in which the transverse momentum dependence of the radiation pattern is averaged out. This energy loss, however, is not a good observable for QCD, because the parton shower is not directly observable due to hadronization. In addition, the QCD bremsstrahlung of hard jets must compete with the hard radiation associated with the jet production. To detect modifications of this hard vacuum bremsstrahlung spectrum due to final state rescattering requires knowledge about the angular distribution of the spectrum. In QCD, the transverse momentum dependence of the LPM-effect is thus indispensable for a quantitative understanding of radiative energy loss.

Recently, Kopeliovich, Schäfer and Tarasov (KST) [27] have used the Furry approximation of the Dirac equation in order to account for the transverse momentum dependence of the radiation spectrum emitted in a multiple scattering process. For the case of QCD bremsstrahlung radiation, they translate their QED results into QCD via an *a posteriori* dipole prescription (5.1). This strategy is frequently used not only for the calculation of the radiative energy loss of high p_t partons [15, 17, 27], but also for the description of nuclear shadowing in the target rest frame [28, 29] and for related problems of diffractive dissociation of virtual photons [30].

As we show in what follows, an extension of the KST-formalism has great potential for the calculation of radiative energy loss in realistic scenarios since (1) it provides a smooth interpolation between the cases of infinitely many and very few rescatterings and (2) it allows to compare QED-inspired calculations of QCD radiative energy loss with perturbative QCD results. The present work focuses on the general formalism, its region of validity, and a qualitative discussion of its generic features. It gives expressions which allow for the numerical calculation of the radiation spectrum as a function of the medium density and extension, but it leaves phenomenological applications to further publications.

Our work is organized as follows. In section II, we derive the starting point of our discussion, the radiation spectrum (2.22). We discuss how a technical complication, the regularization of this spectrum, can be dealt with analytically, and we calculate the corresponding integrated energy loss. Section III focuses on limiting cases of the general radiation formula (2.22). We derive the radiation spectra for $N = 1, 2$ and 3 scatterings and we show that these reproduce the Bethe-Heitler and the factorization limit. In section IV, the dipole approximation of the radiation spectrum (2.22) is discussed. This gives access to true in medium properties of the radiation spectrum which cannot be obtained from an expansion to finite order in the coupling constant. Finally, we discuss in section V how this method can be extended to QCD and how it compares to results from perturbative QCD. Our main results are summarized in the Conclusion.

II. THE LPM-EFFECT IN QED

An expansion of the LPM-radiation cross section in orders of the coupling constant is essentially an expansion in the number of elastic scatterings, since each elastic scattering Mott cross section is proportional to α_{em}^2 . In contrast, a high energy expansion of the solution of the Dirac equation in the presence of an external field takes to leading order in $1/E$ an arbitrary number of elastic scatterings into account. In this section, we derive the corresponding high energy limit of the QED radiation cross section for a hard electron, traversing a medium of

longitudinal density $n(\xi)$. The physics contained in our main result (2.22) will be discussed in the following sections III - V. Our approach in II A parallels to a large extent that of Kopeliovich, Schäfer and Tarasov (KST) in Ref. [27]. We present the derivation in full detail to introduce our notation and to discuss all the approximations involved in the calculation. In contrast to Ref. [27], our radiation cross section (2.22) contains an ϵ -regularization whose treatment is discussed in subsection II B. Then we show that the KST-formalism results in an angular integrated energy loss formula from which modifications to Zakharov's formalism [15, 17] can be obtained.

A. The KST-formalism: Differential cross section in the Furry approximation

We consider a relativistic electron undergoing multiple small-angle scattering in a spatially extended medium, described by an external potential $U(\mathbf{x})$. The angular dependence of the radiation spectrum for emitted photons carrying away a fraction x of the incident electron energy E_1 is given by the differential cross section

$$\frac{d^5\sigma}{d(\ln x) d\mathbf{p}_\perp d\mathbf{k}_\perp} = \frac{\alpha_{em}}{(2\pi)^4} |M_{fi}|^2, \quad (2.1)$$

where \mathbf{k}_\perp and \mathbf{p}_\perp denote the transverse momenta of the photon and outgoing electron, respectively. The radiation amplitude for transversely polarized photons is given in terms of the ingoing and outgoing electron wavefunctions Ψ^- and Ψ^+ ,

$$M_{fi} = \int d^4x \Psi^{-\dagger}(x, p_2) \boldsymbol{\alpha} \cdot \boldsymbol{\epsilon} e^{-\epsilon|z|} e^{i\mathbf{k} \cdot \mathbf{x}} \Psi^+(x, p_1). \quad (2.2)$$

Here, $\boldsymbol{\alpha} = \gamma_0 \boldsymbol{\gamma}$, and $e^{-\epsilon|z|}$ is the adiabatic switching off of the interaction term at large distances. This term plays an important role in what follows since the $\epsilon \rightarrow 0$ limit does not commute with the longitudinal z -integration. The wavefunctions Ψ^\pm solve the Dirac equation in the external potential $U(\mathbf{x})$:

$$\left[i \frac{\partial}{\partial t} - U(\mathbf{x}) - m \gamma_0 + i \boldsymbol{\alpha} \cdot \boldsymbol{\nabla} \right] \Psi(x, p_{1,2}) = 0. \quad (2.3)$$

Following Kopeliovich et al. [27], we rewrite the Dirac equation

$$\begin{aligned} & \left[-\frac{\partial^2}{\partial t^2} - m^2 + \Delta^2 - 2iU(\mathbf{x}) \frac{\partial}{\partial t} \right] \Psi(x, p_{1,2}) \\ &= [-i\boldsymbol{\alpha} \cdot (\boldsymbol{\nabla} U(\mathbf{x})) - U^2(\mathbf{x})] \Psi(x, p_{1,2}). \end{aligned} \quad (2.4)$$

This allows for an expansion to order $1/E$, treating the right hand side as a small perturbation, solving the corresponding homogeneous problem and including in a first

iteration the derivative term $\boldsymbol{\nabla} U(\mathbf{x})$. The result is the Furry approximation [27, 2]:

$$\Psi_F^+(x, p_1) = e^{-iE_1 t + i p_1 z} \hat{D}_1 F^+(\mathbf{x}, \mathbf{p}_1) \frac{u(\mathbf{p}_1)}{\sqrt{2E_1}}, \quad (2.5)$$

$$\Psi_F^-(x, p_2) = e^{-iE_2 t + i p_2 z} \hat{D}_2 F^-(\mathbf{x}, \mathbf{p}_2) \frac{u(\mathbf{p}_2)}{\sqrt{2E_2}}, \quad (2.6)$$

which is exact to order $O(U/E)$ and $O(1/E^2)$. The building blocks of this solution are the differential operators \hat{D}_i and the functions F^\pm whose properties we explain now:

To determine the functions F^\pm , we neglect the second derivative $\partial^2/\partial z^2$ in (2.4). This is allowed since the longitudinal distances in a multiple scattering problem are much larger than the transverse ones. The left hand side of (2.4) reduces then to a two-dimensional Schrödinger equation, with corresponding retarded Green's function

$$\begin{aligned} & \left[i \frac{d}{dz_2} + \frac{\Delta_\perp}{2p} - U(z_2, \mathbf{r}_2) \right] G(z_2, \mathbf{r}_2; z_1, \mathbf{r}_1 | \mathbf{p}) \\ &= i \delta(z_2 - z_1) \delta(\mathbf{r}_2 - \mathbf{r}_1), \end{aligned} \quad (2.7)$$

satisfying $G(z_2 = z_1, \mathbf{r}_2; z_1, \mathbf{r}_1 | \mathbf{p}) = \delta(\mathbf{r}_2 - \mathbf{r}_1)$ and vanishing for $z_1 > z_2$. The functions F^\pm in (2.5), (2.6) are solutions of this two-dimensional Schrödinger equation,

$$\begin{aligned} F^+(\mathbf{x}, \mathbf{p}_1) &= \int d^2\mathbf{r}_1 G(z, \mathbf{r}; z_-, \mathbf{r}_1 | \mathbf{p}_1) F^+(\mathbf{r}_1, z_-, \mathbf{p}_1), \\ F^{-*}(\mathbf{x}, \mathbf{p}_2) &= \int d^2\mathbf{r}_2 F^{-*}(\mathbf{r}_2, z_+, \mathbf{p}_2) G(z_+, \mathbf{r}_2; z, \mathbf{r} | \mathbf{p}_2). \end{aligned}$$

For very early and very late times, i.e. for far forward and far backward longitudinal distances z_+ and z_- respectively, they satisfy the boundary conditions

$$F^+(\mathbf{r}_1, z_-, \mathbf{p}_1) = \exp \left\{ i \mathbf{p}_{1\perp} \cdot \mathbf{r}_1 - i \frac{\mathbf{p}_{1\perp}^2}{2p_1} z_- \right\}, \quad (2.8)$$

$$F^-(\mathbf{r}_2, z_+, \mathbf{p}_2) = \exp \left\{ i \mathbf{p}_{2\perp} \cdot \mathbf{r}_2 - i \frac{\mathbf{p}_{2\perp}^2}{2p_2} z_+ \right\}. \quad (2.9)$$

This ensures that the wavefunctions Ψ_F^\pm approximate plane waves at asymptotic distances. The differential operators \hat{D}_i are obtained by including the derivative term $\boldsymbol{\nabla} U(\mathbf{x})$ of (2.4) in a first iteration of this solution,

$$\begin{aligned} \hat{D}_i &= 1 - i \frac{\boldsymbol{\alpha} \cdot \boldsymbol{\nabla}}{2E_i} - \frac{\boldsymbol{\alpha} \cdot (\mathbf{p}_i - \mathbf{n} p_i)}{2E_i}, \\ \mathbf{n} &= \frac{\mathbf{k}}{k} \quad ; \quad z = \mathbf{n} \cdot \mathbf{x} \quad ; \quad p_i = |\mathbf{p}_i|. \end{aligned} \quad (2.10)$$

We now explain how to obtain from the Furry approximation an explicit expression of the differential radiation cross section (2.1). We work in the ultrarelativistic limit, $E_1 \approx p_1$, $E_2 \approx p_2 = (1-x)p_1$, $\omega = x p_1$. The longitudinal axis is redefined to be parallel to the emitted photon \mathbf{k} , see Figure 1. The transverse momenta of the

ingoing ($\mathbf{p}_{1\perp}$) and outgoing ($\mathbf{p}_{2\perp}$) electron for small x are therefore

$$\mathbf{p}_{1\perp} = \frac{-1}{x} \mathbf{k}_\perp, \quad \mathbf{p}_{2\perp} = \mathbf{p}_\perp - \frac{1-x}{x} \mathbf{k}_\perp, \quad (2.11)$$

$$\mathbf{q}_\perp = \mathbf{p}_{2\perp} - \mathbf{p}_{1\perp} = \mathbf{p}_\perp + \mathbf{k}_\perp. \quad (2.12)$$

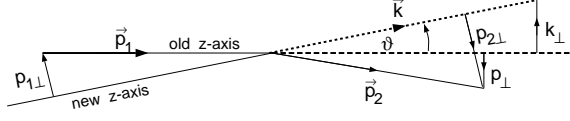


FIG. 1. Choice of the coordinate system in which the new longitudinal z -axis is taken along the radiated photon momentum, see Eqs. (2.11), (2.12).

For the calculation of M_{fi} , we use the following four steps:

- 1) We do the time-integral in (2.2) which ensures energy conservation, $E_1 = E_2 + \omega$.
- 2) We determine the z -dependent phase factor $\bar{q}z$ for (2.2) by observing that the z -dependent phases in (2.5), (2.6) come with the modulus of the spatial momentum $p_i = |\mathbf{p}_i|$. Using energy-momentum conservation, one finds to leading order $1/E$

$$\bar{q} = p_1 - p_2 - k = \frac{x m_e^2}{2(1-x) E_1} \equiv \frac{1}{l_f}. \quad (2.13)$$

The inverse momentum transfer $1/\bar{q}$ is often referred to as photon formation length l_f . However, contributions from transverse energies $\mathbf{k}_\perp^2/2\omega$ dominate the z -dependent phase factor of \mathcal{M}_{fi} , as will be seen below. Hence, l_f gives only a rough upper estimate for the longitudinal size over which interference effects suppress photon emission.

- 3) We absorb in (2.2) the spinor structure of the wavefunctions Ψ_F^+ , Ψ_F^- in the interaction vertex

$$\hat{\Gamma}_r = \sqrt{1-x} u^*(\mathbf{p}_2) \hat{D}_2^* \boldsymbol{\alpha} \cdot \boldsymbol{\epsilon} \hat{D}_1 u(\mathbf{p}_1). \quad (2.14)$$

Depending on the electron spin of the ingoing ($\lambda_e = \pm \frac{1}{2}$) and outgoing ($\lambda_{e'} = \pm \frac{1}{2}$) electron and the photon helicity ($\lambda_\gamma = \pm 1$), this vertex takes the form

$$\begin{aligned} \hat{\Gamma}_r(\lambda_e = \lambda_{e'}, \lambda_\gamma) &= -i \lambda_\gamma [\lambda_\gamma (2-x) + 2 \lambda_e x] \\ &\quad \times \left(\frac{\partial}{\partial r_x} - i \lambda_\gamma \frac{\partial}{\partial r_y} \right), \end{aligned} \quad (2.15)$$

$$\hat{\Gamma}_r(\lambda_e = -\lambda_{e'}, \lambda_\gamma) = 2 m_e x \lambda_\gamma \delta_{\lambda_\gamma, 2\lambda_e}, \quad (2.16)$$

where the spin-flip contribution (2.16) is only non-vanishing for $\lambda_\gamma = 2\lambda_e$. The differential operators in (2.14) act to the right on the two different transverse components of $\mathbf{r} = (r_x, r_y)$. In what follows, we are only interested in the spin- and helicity-averaged combination $\hat{\Gamma}_r \hat{\Gamma}_r^*$, which takes the simple form

$$\hat{\Gamma}_r \hat{\Gamma}_r^* = [4 - 4x + 2x^2] \frac{\partial}{\partial \mathbf{r}} \cdot \frac{\partial}{\partial \mathbf{r}'} + 2m_e^2 x^2. \quad (2.17)$$

- 4) We split up the Green's functions

$$G(z_1, \mathbf{r}_1; z_2, \mathbf{r}_2) = \int d\mathbf{r}' G(z_1, \mathbf{r}_1; z', \mathbf{r}') G(z', \mathbf{r}'; z_2, \mathbf{r}_2)$$

at longitudinal distances z' in such a way that contributions from the amplitude (2.2) and its complex conjugate part can be paired, see eg. (2.18) and Fig. 4.

After these four steps, the radiation probability can be expressed as a Fourier transform over pairs of Green's functions on whose transverse coordinates the interaction vertex (2.17) is acting:

$$\begin{aligned} \langle |M_{fi}|^2 \rangle &= 2 \text{Re} \int d\mathbf{r}_1 d\mathbf{r} d\boldsymbol{\rho} d\mathbf{r}_2 d\mathbf{r}'_1 d\mathbf{r}' d\boldsymbol{\rho}' d\mathbf{r}'_2 \int dz \\ &\quad \times \int_z^\infty dz' e^{-i\mathbf{p}_{2\perp} \cdot (\mathbf{r}_2 - \mathbf{r}'_2) + i\mathbf{p}_{1\perp} \cdot (\mathbf{r}_1 - \mathbf{r}'_1) - i\bar{q}(z' - z)} e^{-\epsilon(|z| + |z'|)} \\ &\quad \times \frac{1}{4p_1^2 (1-x)^2} \langle G(z_+, \mathbf{r}_2; z', \boldsymbol{\rho} | p_2) G^*(z_+, \mathbf{r}'_2; z', \mathbf{r}' | p_2) \rangle \\ &\quad \times \hat{\Gamma}_{-r} \hat{\Gamma}_{r'}^* \langle G(z', \boldsymbol{\rho}; z, \mathbf{r} | p_2) G^*(z', \mathbf{r}'; z, \boldsymbol{\rho}' | p_1) \rangle \\ &\quad \times \langle G(z, \mathbf{r}; z_-, \mathbf{r}_1 | p_1) G^*(z, \boldsymbol{\rho}'; z_-, \mathbf{r}'_1 | p_1) \rangle. \end{aligned} \quad (2.18)$$

To turn this into an explicit expression, it is necessary to i) calculate the averages $\langle \dots \rangle$ over the scattering centers in the medium and ii) evaluate the Green's functions G which are given by path integrals

$$\begin{aligned} G(z', \mathbf{r}'; z, \mathbf{r} | p) &= \\ \int \mathcal{D}\mathbf{r}(\xi) \exp \left\{ \int_z^{z'} d\xi \left[\frac{ip}{2} \dot{\mathbf{r}}^2(\xi) - iU(\mathbf{r}(\xi), \xi) \right] \right\} \end{aligned} \quad (2.19)$$

with boundary conditions $\mathbf{r}(z) = \mathbf{r}$, $\mathbf{r}(z') = \mathbf{r}'$. We show in Appendix A that the in medium averages involved in (2.18) result in a factor which depends on the cross section $\sigma(\boldsymbol{\rho}(\xi))$ times the density $n(\xi)$ of scattering centers as follows

$$\begin{aligned} \left\langle \exp \left\{ i \int_z^{z'} d\xi [U(\mathbf{r}(\xi), \xi) - U(\mathbf{r}'(\xi), \xi)] \right\} \right\rangle \\ = \exp \left\{ - \int_z^{z'} d\xi \Sigma(\xi, [\mathbf{r}(\xi) - \mathbf{r}'(\xi)]) \right\}, \end{aligned} \quad (2.20)$$

$$\Sigma(\xi, \boldsymbol{\rho}(\xi)) = \frac{1}{2} n(\xi) \sigma(\boldsymbol{\rho}(\xi)). \quad (2.21)$$

An explicit expression for $\sigma(\boldsymbol{\rho}(\xi))$, supporting its interpretation as a Mott cross section, is also derived in Appendix A. Most importantly, the resulting expression $\Sigma(\xi, \boldsymbol{\rho}(\xi))$ depends only on the relative distance $\boldsymbol{\rho}(\xi)$ between the paths $\mathbf{r}(\xi)$ and $\mathbf{r}'(\xi)$. As we explain in Appendix B, this makes it possible to carry out a large number of the integrals and path-integrals in (2.18) analytically. One obtains (see Appendix B for further details)

$$\begin{aligned}
\frac{d^5\sigma}{d(\ln x) d\mathbf{p}_\perp d\mathbf{k}_\perp} &= C_{\text{pre}} \text{Re} \int d\boldsymbol{\rho}_2 d\boldsymbol{\rho}_1 \\
&\times \int_{z_-}^{z_+} dz \int_z^{z_+} dz' \exp \{ -i\bar{q}(z' - z) - \epsilon(|z| + |z'|) \} \\
&\times \exp \left\{ - \int_{z_-}^z d\xi \Sigma(\xi, x \boldsymbol{\rho}_1) - \int_{z'}^{z_+} d\xi \Sigma(\xi, x \boldsymbol{\rho}_2) \right\} \\
&\times \exp \left\{ -i x \left(\mathbf{p}_\perp - \frac{1-x}{x} \mathbf{k}_\perp \right) \cdot \boldsymbol{\rho}_2 - i \mathbf{k}_\perp \cdot \boldsymbol{\rho}_1 \right\} \\
&\times \left[g_{\text{nf}} \frac{\partial}{\partial \boldsymbol{\rho}_1} \cdot \frac{\partial}{\partial \boldsymbol{\rho}_2} + g_{\text{sf}} \right] \mathcal{K}(z', \boldsymbol{\rho}_2; z, \boldsymbol{\rho}_1 | \mu). \quad (2.22)
\end{aligned}$$

This differs from the result in [27] by including the regularization $e^{-\epsilon(|z|+|z'|)}$. The physical radiation spectrum is obtained by removing $\epsilon \rightarrow 0$ *after* doing the z and z' -integrations and taking $z_- \rightarrow -\infty$ and $z_+ \rightarrow \infty$. To simplify the notation, we define

$$\mu \equiv E_1(1-x)x, \quad (2.23)$$

which plays the role of mass, and the factor

$$C_{\text{pre}} \equiv \frac{\alpha_{em}}{(2\pi)^4} \frac{2x^2}{E_1^2(1-x)^2}, \quad (2.24)$$

which accounts for a combination of recurring kinematical prefactors. The coefficients of the spin-flip (g_{sf}) and non-flip (g_{nf}) contributions of the interaction vertex (2.17) read

$$g_{\text{nf}} = \frac{4-4x+2x^2}{4x^2}, \quad g_{\text{sf}} = \frac{m_e^2 x^2}{2}. \quad (2.25)$$

The remaining path integral \mathcal{K} in (2.22) is given by

$$\begin{aligned}
&\mathcal{K}(z', \mathbf{r}_c(z'); z, \mathbf{r}_c(z) | \mu) \\
&= \int \mathcal{D}\mathbf{r}_c \exp \left\{ i \int_z^{z'} d\xi \left[\frac{\mu}{2} \dot{\mathbf{r}}_c^2 + i \Sigma(\xi, x \mathbf{r}_c) \right] \right\}. \quad (2.26)
\end{aligned}$$

In this path integral, $\Sigma(\xi, x \mathbf{r}_c)$ plays the role of an imaginary potential, while its physical interpretation is up to a minus sign that of an elastic Mott cross section times the density of scattering centers, cf. equation (A12). Depending on the context, we shall hence refer to Σ as a potential or a cross section.

The following sections are devoted to a study of the differential cross section (2.22). We focus on analytically accessible limiting cases which illustrate the physics contained in (2.22) and we discuss approximations which allow for its numerical analysis.

B. Removing the regularization $\epsilon \rightarrow 0$

The regularization prescription in (2.22) cannot be neglected since the $\epsilon \rightarrow 0$ limit does not commute with

the z - and z' -integrations. This complicates practical applications of (2.22): even if the Green's function \mathcal{K} is known explicitly in some approximation (see sections III and IV below), the expression (2.22) is not suited for numerical calculations since one cannot control numerically the $\epsilon \rightarrow 0$ -limit *after* carrying out the z -integrations.

To solve this problem, we determine the $\epsilon \rightarrow 0$ limit of the radiation spectrum (2.22) analytically. We consider a medium of arbitrary but finite longitudinal extension which is positioned along the longitudinal axis between 0 and the finite distance L . The z - and z' -integrations of (2.22) can be split into six parts,

$$\begin{aligned}
\int_{z_-}^{z_+} \int_z^{z_+} &= \int_{z_-}^0 \int_z^0 + \int_{z_-}^0 \int_0^L + \int_{z_-}^0 \int_L^{z_+} \\
&+ \int_0^L \int_z^L + \int_0^L \int_L^{z_+} + \int_L^{z_+} \int_L^{z_+}. \quad (2.27)
\end{aligned}$$

To shorten the following calculations, we omit the spin-flip contribution g_{sf} to the radiation spectrum. This contribution is negligible in the relativistic limit $m_e \ll E_1$ on which we focus in the following. [If needed, the g_{sf} -contributions to all our results can be recovered without additional technical difficulties.]

The differential cross section receives six contributions which we label according to (2.27) in an obvious way:

$$\begin{aligned}
\frac{d^5\sigma}{d(\ln x) d\mathbf{p}_\perp d\mathbf{k}_\perp} &= C_{\text{pre}} g_{\text{nf}} \\
&\times (I_1 + I_2 + I_3 + I_4 + I_5 + I_6). \quad (2.28)
\end{aligned}$$

Since the medium does not extend outside the interval $[0, L]$, we can replace the in-medium propagator $\mathcal{K}(z', \boldsymbol{\rho}_2; z, \boldsymbol{\rho}_1 | \mu)$ outside $[0, L]$ by the free propagator \mathcal{K}_0 , given in (3.3) below. E.g., for $z_2 > L > z_1$, we can write

$$\begin{aligned}
\mathcal{K}(z_2, \boldsymbol{\rho}_2; z_1, \boldsymbol{\rho}_1 | \mu) &= \int d\mathbf{r} \mathcal{K}_0(z_2, \boldsymbol{\rho}_2; L, \mathbf{r} | \mu) \\
&\times \mathcal{K}(L, \mathbf{r}; z_1, \boldsymbol{\rho}_1 | \mu). \quad (2.29)
\end{aligned}$$

This allows to do all “infinite” integrals $\int_{z_-}^0$ and $\int_L^{z_+}$ in (2.27) analytically. One is left with the “finite” integrals \int_0^L for which the $\epsilon \rightarrow 0$ limit commutes with the z -integration. Doing the z -integrations first, then taking $z_- \rightarrow -\infty$ and $z_+ \rightarrow +\infty$ respectively, and finally adiabatically switching off the regularization, $\epsilon \rightarrow 0$, we find

$$I_1 = (x^2 \mathbf{p}_{1\perp}^2) \int d\mathbf{r} e^{-\int_0^L \Sigma(\xi, x \mathbf{r}) - ix \mathbf{q}_\perp \cdot \mathbf{r}} \mathcal{Z}_1, \quad (2.30)$$

$$I_2 = -\text{Re} \int_0^L dz' e^{-i\bar{q}z'} \int d\mathbf{r} e^{-\int_{z'}^L \Sigma(\xi, x \mathbf{r}) - ix \mathbf{p}_{2\perp} \cdot \mathbf{r}} \mathcal{Z}_2$$

$$\times \int d\bar{\mathbf{r}} e^{i\mathbf{x}\mathbf{p}_{1\perp}\cdot\bar{\mathbf{r}}} x\mathbf{p}_{1\perp} \cdot \frac{\partial}{\partial \mathbf{r}} \mathcal{K}(z', \mathbf{r}; 0, \bar{\mathbf{r}}|\mu), \quad (2.31)$$

$$I_3 = (x\mathbf{p}_{1\perp}) \cdot (x\mathbf{p}_{2\perp}) \text{Re} \int d\mathbf{r}_1 d\mathbf{r}_2 e^{-i\mathbf{x}\mathbf{p}_{2\perp}\cdot\mathbf{r}_2} \times e^{i\mathbf{x}\mathbf{p}_{1\perp}\cdot\mathbf{r}_1} \mathcal{K}(L, \mathbf{r}_2; 0, \mathbf{r}_1|\mu) \mathcal{Z}_3 e^{-iL\bar{q}}, \quad (2.32)$$

$$I_4 = \text{Re} \int_0^L dz \int_z^L dz' \int d\mathbf{r}_1 d\mathbf{r}_2 e^{-i\mathbf{x}\mathbf{p}_{2\perp}\cdot\mathbf{r}_2} e^{i\mathbf{x}\mathbf{p}_{1\perp}\cdot\mathbf{r}_1} \times e^{-\int_0^z \Sigma(\xi, x\mathbf{r}_1) - \int_{z'}^L \Sigma(\xi, x\mathbf{r}_2)} e^{-i\bar{q}(z'-z)} \times \frac{\partial}{\partial \mathbf{r}_1} \cdot \frac{\partial}{\partial \mathbf{r}_2} \mathcal{K}(z', \mathbf{r}_2; z, \mathbf{r}_1|\mu), \quad (2.33)$$

$$I_5 = \text{Re} \int_0^L dz e^{i\bar{q}(z-L)} \int d\mathbf{r} e^{-\int_0^z \Sigma(\xi, x\mathbf{r}) + i\mathbf{x}\mathbf{p}_{1\perp}\cdot\mathbf{r}} \mathcal{Z}_5 \times \int d\bar{\mathbf{r}} e^{-i\mathbf{x}\mathbf{p}_{2\perp}\cdot\bar{\mathbf{r}}} x\mathbf{p}_{2\perp} \cdot \frac{\partial}{\partial \mathbf{r}} \mathcal{K}(L, \bar{\mathbf{r}}; z, \mathbf{r}|\mu), \quad (2.34)$$

$$I_6 = (x^2 \mathbf{p}_{2\perp}^2) \int d\mathbf{r} e^{-\int_0^L \Sigma(\xi, x\mathbf{r}) - i\mathbf{x}\mathbf{q}_\perp \cdot \mathbf{r}} \mathcal{Z}_6. \quad (2.35)$$

Here, the factors \mathcal{Z}_i contain the explicit solutions of those z -integrals which extend to z_+ or z_- respectively. Using the notational shorthands

$$Q_1 = \frac{x^2 \mathbf{p}_{1\perp}^2}{2\mu} + \bar{q} = \frac{x^2 (\mathbf{p}_{1\perp}^2 + m_e^2)}{2\mu}, \quad (2.36)$$

$$Q_2 = \frac{x^2 (\mathbf{p}_{2\perp}^2 + m_e^2)}{2\mu}, \quad (2.37)$$

we obtain

$$\mathcal{Z}_1 = \text{Re} \int_{z_-}^0 dz \int_z^0 dz' e^{-iQ_1(z'-z) - \epsilon(|z|+|z'|)} = \frac{1}{2Q_1^2}, \quad (2.38)$$

and analogously,

$$\mathcal{Z}_2 = \frac{1}{Q_1}, \quad \mathcal{Z}_3 = -\frac{1}{Q_1 Q_2}, \quad (2.39)$$

$$\mathcal{Z}_5 = \frac{1}{Q_2}, \quad \mathcal{Z}_6 = \frac{1}{2Q_2^2}. \quad (2.40)$$

The differential radiation spectrum (2.28) given by the equations (2.30) - (2.40) is suitable for a numerical evaluation since the $\epsilon \rightarrow 0$ -limit is taken. Previous numerical investigations [27] of (2.22) were based on a non-regularized expression which did not include the term $e^{-\epsilon(|z|+|z'|)}$ in the integrand. The difference to the above results is found by determining the above z -integrals without regularization:

$$\mathcal{Z}_1^{nr} = \text{Re} \int_{z_-}^0 dz \int_z^0 dz' e^{-iQ_1(z'-z)}$$

$$= 2\mathcal{Z}_1 (1 - \cos\{Q_1 z_-\}), \quad (2.41)$$

$$\mathcal{Z}_2^{nr} = \mathcal{Z}_2 (1 - \exp\{iQ_1 z_-\}), \quad (2.42)$$

$$\mathcal{Z}_3^{nr} = \mathcal{Z}_3 (1 - \exp\{iQ_1 z_-\}) \times (1 - \exp\{iQ_2(z_+ - L)\}), \quad (2.43)$$

$$\mathcal{Z}_5^{nr} = \mathcal{Z}_5 (1 - \exp\{iQ_2(z_+ - L)\}), \quad (2.44)$$

$$\mathcal{Z}_6^{nr} = 2\mathcal{Z}_6 (1 - \cos\{Q_2(z_+ - L)\}). \quad (2.45)$$

The differential cross-section (2.22) can be related to the unregularized one $\sigma^{(nr)}$:

$$\frac{d^5\sigma}{d(\ln x) d\mathbf{p}_\perp d\mathbf{k}_\perp} = \frac{d^5\sigma^{(nr)}}{d(\ln x) d\mathbf{p}_\perp d\mathbf{k}_\perp} \left\{ -\frac{C_{\text{pre}}}{2} \int d\boldsymbol{\rho} \exp \left\{ -\int_{z_-}^{z_+} \Sigma(\xi, x\boldsymbol{\rho}) - i\mathbf{x}\mathbf{q}_\perp \cdot \boldsymbol{\rho} \right\} \times \left[\frac{(x^2 \mathbf{p}_{1\perp}^2)}{Q_1} + \frac{(x^2 \mathbf{p}_{2\perp}^2)}{Q_2} \right] + \Theta_{\text{corr}}^{\text{osc}}[z_-, z_+] \right\}. \quad (2.46)$$

Here, the correction term $\Theta_{\text{corr}}^{\text{osc}}[z_-, z_+]$ summarizes those oscillating contributions which vanish if one averages suitably in a numerical calculation over the boundaries z_- and z_+ of the longitudinal integration. In addition, there are two terms which do not depend on the boundaries z_- , z_+ . They stem from the terms \mathcal{Z}_1^{nr} and \mathcal{Z}_6^{nr} which differ by an overall factor 2 from the regularized expressions \mathcal{Z}_1 , \mathcal{Z}_6 . These terms provide the proper subtraction of the Weizsäcker-Williams fields of the ingoing and outgoing electron. As will become clear below, they are non-negligible, and ensure e.g. the consistency of (2.22) with the Bethe-Heitler spectrum in the appropriate limiting cases.

C. Integrated energy loss cross section

The total energy loss cross section is calculated by integrating (2.22) over transverse momenta. To this aim, we rewrite the differential cross section as a function of the relative momentum transfer $\mathbf{q}_\perp = \mathbf{k}_\perp + \mathbf{p}_\perp$ and the transverse momentum \mathbf{k}_\perp of the emitted photon. Since there is no kinematical boundary on \mathbf{q}_\perp , the integration over the transverse momentum of the electron is simple:

$$\frac{d^3\sigma}{d(\ln x) d\mathbf{k}_\perp} = (2\pi)^2 \frac{C_{\text{pre}}}{x^2} \text{Re} \int d\boldsymbol{\rho}_1 \int_{z_-}^{z_+} dz \int_z^{z_+} dz' e^{-i\bar{q}(z'-z)} \times \exp \left\{ -\epsilon(|z|+|z'|) - \int_{z_-}^z d\xi \Sigma(\xi, x\boldsymbol{\rho}_1) - i\mathbf{k}_\perp \cdot \boldsymbol{\rho}_1 \right\} \times \left[g_{\text{nf}} \frac{\partial}{\partial \boldsymbol{\rho}_1} \cdot \frac{\partial}{\partial \boldsymbol{\rho}_2} + g_{\text{sf}} \right] \mathcal{K}(z', \boldsymbol{\rho}_2 = 0; z, \boldsymbol{\rho}_1|\mu). \quad (2.47)$$

The integration over the photon transverse momentum is more complicated due to the finite kinematical boundaries for the photon, $|\mathbf{k}_\perp| < \omega = x E_1$:

$$\begin{aligned}
\frac{d\sigma}{d(\ln x)} &= \int_0^\omega d\mathbf{k}_\perp \frac{d^3\sigma}{d(\ln x) d\mathbf{k}_\perp} \cdot \\
&= \frac{\alpha_{\text{em}}}{(2\pi)^2} \frac{2 \text{Re}}{E_1^2 (1-x)^2} \int d\boldsymbol{\rho}_1 \frac{2\pi\omega J_1(\omega\rho_1)}{\rho_1} \\
&\quad \times \int_{z_-}^{z_+} dz \int_z^{z_+} dz' e^{-i\bar{q}(z'-z) - \epsilon(|z|+|z'|)} \\
&\quad \times \exp \left\{ - \int_{z_-}^z \Sigma(\xi, x\boldsymbol{\rho}_1) \right\} \left[g_{\text{nf}} \frac{\partial}{\partial \boldsymbol{\rho}_1} \cdot \frac{\partial}{\partial \boldsymbol{\rho}_2} + g_{\text{sf}} \right] \\
&\quad \times \mathcal{K}(z', \boldsymbol{\rho}_2 = 0; z, \boldsymbol{\rho}_1 | \mu) . \tag{2.48}
\end{aligned}$$

It is interesting to compare this energy loss formula to that derived by Zakharov [15, 17]:

$$\begin{aligned}
\frac{d\sigma^{(\text{zak})}}{d(\ln x)} &= \alpha_{\text{em}} \frac{2 \text{Re}}{E_1^2 (1-x)^2} \int_{z_-}^{z_+} dz \int_z^{z_+} dz' e^{-i\bar{q}(z'-z)} \\
&\quad \times \left[g_{\text{nf}} \frac{\partial}{\partial \boldsymbol{\rho}_1} \cdot \frac{\partial}{\partial \boldsymbol{\rho}_2} + g_{\text{sf}} \right] \\
&\quad \times [\mathcal{K}(z', 0; z, 0 | \mu) - \mathcal{K}_0(z', 0; z, 0 | \mu)] . \tag{2.49}
\end{aligned}$$

Here, \mathcal{K}_0 is the free, non-interacting path integral, given explicitly in (3.3) below. If we had ignored the kinematical boundary, extending the k_\perp -integration in (2.48) up to infinity, we would have regained the expression of Zakharov except for the term proportional to \mathcal{K}_0 .

We note that Zakharov's arguments leading to (2.49) are very different from our derivation of (2.48). The transverse momentum dependence of the radiation enters in no intermediate step of his calculation [17]. Also, the \mathcal{K}_0 -term in (2.49) does not result from a derivation: it is rather subtracted *a posteriori* as a 'renormalization prescription' in order to cancel a singularity in the integrand of (2.49) for small $(z' - z)$. In this sense, our derivation differs from Zakharov's result (2.49) by: i) taking the finite phase space of the emitted photon properly into account, ii) containing a proper ϵ -regularization of the radiation amplitude and iii) not employing a subtraction of a singular contribution *a posteriori*.

III. THE LOW OPACITY EXPANSION FOR THIN TARGETS

Information about the target medium enters the radiation cross section (2.22) via the product $\Sigma(\xi, \boldsymbol{\rho})$, which measures the elastic cross section times the density of scattering centers in the medium. Since $\Sigma(\xi, \boldsymbol{\rho}) \propto \alpha_{\text{em}}^2 n(\xi)$, an expansion of (2.22) in powers of α_{em}^2 is an expansion in powers of the opacity $\mathcal{T} \sigma_{\text{eff}}$, where σ_{eff} is the effective elastic single scattering cross section and

$$\mathcal{T} = \int_0^L d\xi n(\xi) . \tag{3.1}$$

$\mathcal{T} \sigma_{\text{eff}}$ measures the average number of scatterings for an electron traversing a medium of length L . Since the elastic cross section in (2.22) is not a geometrical quantity but depends on the integration variables, our expansion of (2.22) will be formally in powers of $\alpha_{\text{em}}^2 \mathcal{T}$, and we shall refer by a slight abuse of language to \mathcal{T} as opacity. Of course, after all integrals are done, each power of $\alpha_{\text{em}}^2 \mathcal{T}$ will be accompanied by a power of the elastic cross section. The N -th term in this expansion of (2.22) is of order $\alpha_{\text{em}}^{(2N+1)} \mathcal{T}^N$ and corresponds to the multiple scattering off exactly N external potentials. An expansion in the opacity \mathcal{T} is thus an expansion in the number of rescatterings.

Below, we study this low opacity expansion of the radiation spectrum up to third order. This leads for equation (2.22) to a number of consistency checks which any radiation spectrum including in medium effects should satisfy. Moreover, this provides the basis for a discussion of the corresponding QCD radiation spectrum in section V.

A. Bethe-Heitler cross section as a low density limit

The derivation of the radiation spectrum (2.22) relies on the approximation that the distribution of scattering centers in the medium can be described by the average (2.20). This uses explicitly that the size of the medium is much larger than the Debye radius of a single scattering potential. A priori, it may hence seem unclear to what extent one can still recover from (2.22) the correct radiation spectrum for a single scattering process where the extension of the potential is the extension of the target. However, in the low opacity limit, when the distance between scattering centers is much larger than the photon formation length, multiple scattering should not affect the radiation pattern. The radiation spectrum should converge to the single scattering Bethe-Heitler cross section times the opacity factor \mathcal{T} . Deriving this is an important consistency check for our formalism.

Our expansion of the integrand of the cross section (2.22) in powers of $\Sigma(\xi, \boldsymbol{\rho}) \propto \alpha_{\text{em}}^2 n(\xi)$, uses the corresponding expansion of the path integral

$$\begin{aligned}
\mathcal{K}(z', \boldsymbol{\rho}_2; z, \boldsymbol{\rho}_1) &= \mathcal{K}_0(z', \boldsymbol{\rho}_2; z, \boldsymbol{\rho}_1) \\
&- \int_z^{z'} d\bar{z} \int d\boldsymbol{\rho} \mathcal{K}_0(z', \boldsymbol{\rho}_2; \bar{z}, \boldsymbol{\rho}) \Sigma(\bar{z}, x\boldsymbol{\rho}) \mathcal{K}_0(\bar{z}, \boldsymbol{\rho}; z, \boldsymbol{\rho}_1) \\
&+ \int_z^{z'} d\bar{z}_1 \int_{\bar{z}_1}^{z'} d\bar{z}_2 \int d\bar{\mathbf{r}}_1 d\bar{\mathbf{r}}_2 \mathcal{K}_0(z', \boldsymbol{\rho}_2; \bar{z}_2, \bar{\mathbf{r}}_2) \Sigma(\bar{z}_2, x\bar{\mathbf{r}}_2) \\
&\quad \times \mathcal{K}(\bar{z}_2, \bar{\mathbf{r}}_2; \bar{z}_1, \bar{\mathbf{r}}_1) \Sigma(\bar{z}_1, x\bar{\mathbf{r}}_1) \mathcal{K}_0(\bar{z}_1, \bar{\mathbf{r}}_1; z, \boldsymbol{\rho}_1) , \tag{3.2}
\end{aligned}$$

where from now on, we suppress the explicit μ -dependence in \mathcal{K} and in the corresponding free Green's function \mathcal{K}_0 ,

$$\mathcal{K}_0(z', \rho_2; z, \rho_1) = \frac{\mu}{2\pi i (z' - z)} \exp \left\{ \frac{i\mu (\rho_1 - \rho_2)^2}{2(z' - z)} \right\}. \quad (3.3)$$

From the two potentials in the third line of (2.22) and from the propagator \mathcal{K} , the radiation spectrum (2.22) receives three contributions to order $O(\alpha_{\text{em}}^3 \mathcal{T})$:

$$\frac{d^5\sigma}{d(\ln x) d\mathbf{p}_\perp d\mathbf{k}_\perp} \Big|_{O(\alpha_{\text{em}}^3 \mathcal{T})} = C_{\text{pre}} g_{\text{nf}} (I_1 + I_2 + I_3), \quad (3.4)$$

$$I_1 = -\text{Re} \int_{z_-}^{z_+} dz \int_z^{z_+} dz' e^{-i\bar{q}(z'-z) - \epsilon(|z| + |z'|)} \int d\rho_2 d\rho_1 \times e^{i x \mathbf{p}_{2\perp} \cdot \rho_2 - i x \mathbf{p}_{1\perp} \cdot \rho_1} \int_{z_-}^z \Sigma(\xi, x \rho_1) \kappa_1(\rho_1, \rho_2), \quad (3.5)$$

$$I_2 = -\text{Re} \int_{z_-}^{z_+} dz \int_z^{z_+} dz' e^{-i\bar{q}(z'-z) - \epsilon(|z| + |z'|)} \int d\rho_2 d\rho_1 \times e^{i x \mathbf{p}_{2\perp} \cdot \rho_2 - i x \mathbf{p}_{1\perp} \cdot \rho_1} \int_{z'}^{z_+} \Sigma(\xi, x \rho_1) \kappa_1(\rho_1, \rho_2), \quad (3.6)$$

$$I_3 = -\text{Re} \int_{z_-}^{z_+} dz \int_z^{z_+} dz' e^{-i\bar{q}(z'-z)} \int d\rho_2 d\rho_1 \times e^{i x \mathbf{p}_{2\perp} \cdot \rho_2 - i x \mathbf{p}_{1\perp} \cdot \rho_1} \kappa_2(\rho_1, \rho_2). \quad (3.7)$$

Here, κ_1 and κ_2 denote the derivatives of the zeroth and first order contributions to the propagator (3.2),

$$\kappa_1(\rho_1, \rho_2) = \frac{\partial}{\partial \rho_1} \cdot \frac{\partial}{\partial \rho_2} \mathcal{K}_0(z', \rho_2; z, \rho_1). \quad (3.8)$$

$$\kappa_2(\rho_1, \rho_2) = \frac{\partial}{\partial \rho_1} \cdot \frac{\partial}{\partial \rho_2} \int_z^{z'} d\bar{z} \int d\rho \mathcal{K}_0(z', \rho_2; \bar{z}, \rho) \times \Sigma(\bar{z}, x \rho) \mathcal{K}_0(\bar{z}, \rho; z, \rho_1). \quad (3.9)$$

We consider a medium of finite longitudinal extension L and homogeneous density $n(\xi) = n_0$. Then, all integrals in (3.5) - (3.7) can be done analytically. Taking the limit $\epsilon \rightarrow 0$ after the z -integrations, we arrive at

$$I_1 = -L n_0 \frac{x^2 \mathbf{p}_{2\perp}^2}{2 Q_2^2} \frac{(2\pi)^2}{x^2} \tilde{\Sigma}(\mathbf{q}_\perp), \quad (3.10)$$

$$I_2 = -L n_0 \frac{x^2 \mathbf{p}_{1\perp}^2}{2 Q_1^2} \frac{(2\pi)^2}{x^2} \tilde{\Sigma}(\mathbf{q}_\perp), \quad (3.11)$$

$$I_3 = -L n_0 \frac{x^2 \mathbf{p}_{2\perp} \cdot \mathbf{p}_{1\perp}}{Q_1 Q_2} \frac{(2\pi)^2}{x^2} \tilde{\Sigma}(\mathbf{q}_\perp). \quad (3.12)$$

The result is particularly transparent in the relativistic limit, when all mass dependencies can be neglected and

$\bar{q} \approx 0$. For a medium characterized by a set of Yukawa potentials with electric charge Ze and Debye screening mass M (see Appendix A for a derivation),

$$-\tilde{\Sigma}(\mathbf{q}_\perp) \Big|_{\mathbf{q}_\perp \neq 0} = \frac{4 Z^2 \alpha_{\text{em}}^2}{(M^2 + \mathbf{q}_\perp^2)^2} \quad (3.13)$$

denotes the elastic scattering cross section with \mathbf{q}_\perp given by (2.12). The three terms (3.10)-(3.12) then combine to

$$\frac{d^5\sigma}{d(\ln x) d\mathbf{p}_\perp d\mathbf{k}_\perp} \Big|_{O(\alpha_{\text{em}}^3 \mathcal{T})} = \frac{Z^2 \alpha_{\text{em}}^3}{(2\pi)^2} \frac{16 x^2}{(M^2 + \mathbf{q}_\perp^2)^2} \frac{\mathbf{q}_\perp^2}{\mathbf{k}_\perp^2 (\mathbf{k}_\perp - x \mathbf{q}_\perp)^2} \mathcal{T}. \quad (3.14)$$

This is the high-energy limit of the Bethe-Heitler radiation cross section for scattering off a Yukawa potential times the opacity factor $\mathcal{T} = L n_0$. The exact result [see e.g. equation (5.150) of Ref. [31] in the coordinate system Fig. 1 used here.] differs from the above approximation only by terms of order $1 + O(q^2/E^2)$ and $1 + O(x^2)$. The main properties of the QED radiation spectrum are seen clearly from (3.14). The spectrum vanishes for vanishing momentum transfer $q_\perp \rightarrow 0$, it shows the x^2 -dependence characteristic for the QED radiation spectrum peaking at forward rapidity, and it shows the correct $1/\mathbf{k}_\perp^2 (\mathbf{k}_\perp - x \mathbf{q}_\perp)^2$ dependence.

We mention as an aside that the evaluation of the cross section (3.4) without regularization prescription leads to terms I_1 and I_2 which are a factor 2 larger while the interference term remains unchanged. The ϵ -regularization of (2.22) is thus necessary to regain the Bethe-Heitler spectrum.

B. Low N multiple scatterings

In complete analogy to the derivation of the Bethe-Heitler limit, one can expand the cross section (2.22) to second order. All contributions to the radiation cross section depend now on the product of two elastic Mott cross sections $\tilde{\Sigma}$, whose combined momentum transfers sum up to \mathbf{q}_\perp . For this we introduce the shorthand

$$\int d\mathcal{V}^2(\mathbf{q}_\perp) \equiv \int d\mathbf{q}_{1\perp} d\mathbf{q}_{2\perp} \tilde{\Sigma}(\mathbf{q}_{1\perp}) \tilde{\Sigma}(\mathbf{q}_{2\perp}) \times \frac{(2\pi)^2}{x^2} \delta^{(2)}(\mathbf{q}_\perp - \mathbf{q}_{1\perp} - \mathbf{q}_{2\perp}). \quad (3.15)$$

Also, we introduce shorthands for the transverse momenta and the corresponding transverse energies,

$$\begin{aligned} \mathbf{u}_1 &= x \mathbf{p}_{1\perp}, & \mathbf{u}_2 &= x \mathbf{p}_{2\perp}, \\ \mathbf{u}_m &= x (\mathbf{p}_{1\perp} + \mathbf{q}_{1\perp}) = x (\mathbf{p}_{2\perp} - \mathbf{q}_{2\perp}), \\ Q_1 &= \frac{\mathbf{u}_1^2}{2\mu}, & Q_m &= \frac{\mathbf{u}_m^2}{2\mu}, & Q_2 &= \frac{\mathbf{u}_2^2}{2\mu}. \end{aligned}$$

The second order contribution of the radiation spectrum (2.22) consists of six terms. After integrating out all transverse coordinates, it takes the form

$$\begin{aligned} \frac{d^5\sigma}{d(\ln x) d\mathbf{p}_\perp d\mathbf{k}_\perp} \Big|_{O(\alpha_{\text{em}}^5 \mathcal{T}^2)} &= C_{\text{pre}} g_{\text{nf}} \int d\mathcal{V}^2(\mathbf{q}_\perp) \\ &\times \left[\frac{1}{2} \mathbf{u}_1^2 \mathcal{Z}_1^{(2)} + \mathbf{u}_m^2 \mathcal{Z}_2^{(2)} + \frac{1}{2} \mathbf{u}_2^2 \mathcal{Z}_3^{(2)} + \mathbf{u}_1 \cdot \mathbf{u}_2 \mathcal{Z}_4^{(2)} \right. \\ &\quad \left. + \mathbf{u}_m \cdot \mathbf{u}_2 \mathcal{Z}_5^{(2)} + \mathbf{u}_m \cdot \mathbf{u}_1 \mathcal{Z}_6^{(2)} \right] n_0^2. \end{aligned} \quad (3.16)$$

The first three terms stem from the expansion of the exponential term $\exp \left\{ -\int_{z_-}^z \Sigma - \int_{z'}^{z_+} \Sigma \right\}$ in (2.22) to second order in Σ , the fourth term is from the second order expansion of the Green's function \mathcal{K} , and the remaining two terms are contributions from the first order in \mathcal{K} times the first order of the exponential term. The variables $\mathcal{Z}_i^{(2)}$ stand for the remaining longitudinal integrals over phase factors. In general, they are involved, e.g.

$$\begin{aligned} \mathcal{Z}_4^{(2)} &= \text{Re} \int_{z_-}^{z_+} dz \int_z^{z_+} dz' e^{-\epsilon(|z|+|z'|)} \int_z^{z'} d\bar{z}_1 \frac{n(\bar{z}_1)}{n_0} \int_{\bar{z}_1}^{z'} d\bar{z}_2 \frac{n(\bar{z}_2)}{n_0} \\ &\times e^{-iQ_2(z' - \bar{z}_2) - iQ_m(\bar{z}_2 - \bar{z}_1) - iQ_1(\bar{z}_1 - z)}. \end{aligned} \quad (3.17)$$

For a medium of homogeneous density n_0 and finite length L , they reduce to very simple forms:

$$\mathcal{Z}_1^{(2)} = \frac{L^2}{2Q_1^2}, \quad (3.18)$$

$$\mathcal{Z}_2^{(2)} = \frac{\cos(LQ_m) - 1 + \frac{1}{2}L^2 Q_m^2}{Q_m^4}, \quad (3.19)$$

$$\mathcal{Z}_3^{(2)} = \frac{L^2}{2Q_2^2}, \quad (3.20)$$

$$\mathcal{Z}_4^{(2)} = \frac{\cos(LQ_m) - 1}{Q_1 Q_2 Q_m^2}, \quad (3.21)$$

$$\mathcal{Z}_5^{(2)} = -\frac{\cos(LQ_m) - 1 + \frac{1}{2}L^2 Q_m^2}{Q_2 Q_m^3}, \quad (3.22)$$

$$\mathcal{Z}_6^{(2)} = -\frac{\cos(LQ_m) - 1 + \frac{1}{2}L^2 Q_m^2}{Q_1 Q_m^3}. \quad (3.23)$$

From this, we read off simple limiting cases: In the limit of a very thin target of fixed opacity, we can move the two scattering centers so close together that the photon cannot resolve them. The spectrum is then indistinguishable from a single scattering process

$$\begin{aligned} \lim_{L \rightarrow 0} \frac{d^5\sigma}{d(\ln x) d\mathbf{p}_\perp d\mathbf{k}_\perp} \Big|_{O(\alpha_{\text{em}}^5 \mathcal{T}^2)}^{\mathcal{T} \text{ fixed}} \\ = C_{\text{pre}} g_{\text{nf}} \frac{\mathcal{T}^2}{4} \left(\frac{\mathbf{u}_1}{Q_1} - \frac{\mathbf{u}_2}{Q_2} \right)^2 \int d\mathcal{V}^2(\mathbf{q}_\perp). \end{aligned} \quad (3.24)$$

This is the coherent factorization limit that corresponds to one single effective Bethe-Heitler radiation spectrum

which depends only on the initial and final momenta. The characteristic momentum dependence of the Bethe-Heitler radiation spectrum (3.14) is now combined with the convolution of two Mott cross sections (3.15). The first L -dependent correction to this factorization limit is proportional to L^2 and takes the form

$$\begin{aligned} C_{\text{pre}} g_{\text{nf}} \frac{\mathcal{T}^2}{24} L^2 \int d\mathcal{V}^2(\mathbf{q}_\perp) Q_m^2 \\ \times \left[2 \frac{\mathbf{u}_m^2}{Q_m^2} + \frac{\mathbf{u}_1 \cdot \mathbf{u}_2}{Q_1 Q_2} + \frac{\mathbf{u}_m \cdot \mathbf{u}_2}{Q_m Q_2} + \frac{\mathbf{u}_m \cdot \mathbf{u}_1}{Q_1 Q_m} \right], \end{aligned} \quad (3.25)$$

which is mainly of formal interest since the \mathbf{q}_\perp -integral diverges logarithmically.

In the opposite limit, $L \rightarrow \infty$, we can study for fixed opacity $\mathcal{T} = L n_0$ the case of two well-separated scattering centers:

$$\begin{aligned} \lim_{L \rightarrow \infty} \frac{d^5\sigma}{d(\ln x) d\mathbf{p}_\perp d\mathbf{k}_\perp} \Big|_{O(\alpha_{\text{em}}^5 \mathcal{T}^2)}^{\mathcal{T} \text{ fixed}} &= C_{\text{pre}} g_{\text{nf}} \int d\mathcal{V}^2(\mathbf{q}_\perp) \\ &\times \frac{\mathcal{T}^2}{4} \left[\left(\frac{\mathbf{u}_1}{Q_1} - \frac{\mathbf{u}_m}{Q_m} \right)^2 + \left(\frac{\mathbf{u}_m}{Q_m} - \frac{\mathbf{u}_2}{Q_2} \right)^2 \right]. \end{aligned} \quad (3.26)$$

This is the incoherent Bethe-Heitler limit in which the radiation spectrum is the sum of two independent Bethe-Heitler contributions associated with the scattering off the first and the second external potential with momentum transfers $\mathbf{q}_{1\perp}$ and $\mathbf{q}_{2\perp}$, respectively. It provides the starting point for a comparison of the corresponding QCD radiation spectrum with a full $N = 2$ perturbative calculation in section V.

The pattern emerging in this expansion to second order in the opacity is fully confirmed in the case of $N = 3$ scattering centers. In Appendix C, we derive the corresponding radiation cross section and check the Bethe-Heitler and factorization limit.

IV. DIPOLE APPROXIMATION FOR TARGETS OF ARBITRARY EXTENSION

To calculate the radiation spectrum (2.22) to all orders in opacity, an approximation scheme for the path integral \mathcal{K} is needed. The low opacity expansion, studied in section III, becomes rapidly more complicated for increasing number of scattering centers. It is only useful for the description of ultrathin media where very few elastic scatterings have to be taken into account. For the generic case of a hard projectile particle undergoing many small angle scatterings, the dipole approximation of \mathcal{K} is standard [15, 17, 16, 27, 30, 32].

This dipole approximation is based on the observation that for small transverse distances $\rho = |\boldsymbol{\rho}|$, the cross section $\sigma(\rho)$ of the Yukawa potential (A11) has a leading quadratic dependence: [15]

$$\sigma(\rho) \approx C(\rho) \rho^2, \quad (4.1)$$

$$C(\rho) = 4\pi (Z\alpha_{\text{em}})^2 \left[\log\left(\frac{2}{M\rho}\right) + \frac{1-2\gamma}{2} \right], \quad (4.2)$$

where $\gamma = 0.577$ denotes Euler's constant. The main contribution to the radiation spectrum (2.22) comes from small values of ρ , where $C(\rho x)$ shows only a slow logarithmic dependence on ρ and can be approximated by a constant, $C = C(\rho_{\text{eff}} x)$. For a quadratic dependence $\sigma(\rho) = C\rho^2$, where this logarithmic dependence is weak enough to be neglected, the path integral \mathcal{K} in (2.26) is that of a harmonic oscillator [15]

$$\begin{aligned} \mathcal{K}_{\text{osz}}(z_2, \mathbf{r}_2; z_1, \mathbf{r}_1) &= \frac{\mu\Omega}{2\pi i \sin(\Omega\Delta z)} \\ &\times \exp\left\{ \frac{i\mu\Omega [(\mathbf{r}_1^2 + \mathbf{r}_2^2) \cos(\Omega\Delta z) - 2\mathbf{r}_1 \cdot \mathbf{r}_2]}{2 \sin(\Omega\Delta z)} \right\} \end{aligned} \quad (4.3)$$

with the oscillator frequency

$$\Omega = \frac{1-i}{\sqrt{2}} \sqrt{\frac{nCx^2}{\mu}}. \quad (4.4)$$

In the following, we exploit the consequences of this approximation.

A. The general expression: Non-analyticity in the coupling constant

In section IIB, we have determined the six contributions (2.30) - (2.35) to the radiation spectrum (2.22). In the dipole approximation, the transverse integrations in (2.30) - (2.35) reduce to Gaussian integrals and can be done analytically. Here we discuss the resulting expression

$$\frac{d^5\sigma}{d(\ln x) d\mathbf{p}_\perp d\mathbf{k}_\perp} = C_{\text{pre}} g_{\text{nf}} \sum_{j=1}^6 I_j^{(\text{osc})}, \quad (4.5)$$

obtained from (2.28). For three of the six terms $I_j^{(\text{osc})}$, all integrals can be done analytically:

$$I_1^{(\text{osc})} = \frac{1}{2} \frac{\mathbf{p}_{1\perp}^2}{Q_1^2} \frac{2\pi}{nCL} \exp\left\{ -\frac{\mathbf{q}_\perp^2}{2nCL} \right\}, \quad (4.6)$$

$$I_6^{(\text{osc})} = \frac{1}{2} \frac{\mathbf{p}_{2\perp}^2}{Q_2^2} \frac{2\pi}{nCL} \exp\left\{ -\frac{\mathbf{q}_\perp^2}{2nCL} \right\}, \quad (4.7)$$

$$\begin{aligned} I_3^{(\text{osc})} &= \frac{x^2 \mathbf{p}_{1\perp} \cdot \mathbf{p}_{2\perp}}{Q_1 Q_2} \text{Re} e^{-iL\bar{q}} \\ &\times \exp\left\{ -\frac{ix^2(1-\cos(\Omega L))}{2\mu\Omega \sin(\Omega L)} (\mathbf{p}_{2\perp}^2 - \mathbf{p}_{1\perp}^2) \right\} \\ &\times \frac{2i\pi}{\mu\Omega \sin(\Omega L)} \exp\left\{ \frac{ix^2 \mathbf{q}_\perp^2}{2\mu\Omega \sin(\Omega L)} \right\}. \end{aligned} \quad (4.8)$$

These terms show a characteristic dependence on the coupling constant: in the dipole approximation, C is constant and measures the size of the elastic single scattering Mott cross section, see Eq. (4.2). Thus, C and Ω^2 are proportional to α_{em}^2 , and the three terms I_1 , I_6 and I_3 are non-analytic in the coupling constant. For small α_{em}^2 , their leading dependence is $\alpha_{\text{em}}^{-2} \times \exp\{O(\alpha_{\text{em}}^{-2})\}$. We show in the next subsection that these contributions combine to a radiation cross section with a leading dependence $\alpha_{\text{em}} \times \exp\{O(\alpha_{\text{em}}^{-2})\}$. The factor

$$\exp\left\{ -\frac{\mathbf{q}_\perp^2}{2nCL} \right\}, \quad (4.9)$$

responsible for the remaining non-analyticity of the radiation cross section has an intuitive physical interpretation as Molière \mathbf{q}_\perp -broadening. This broadening is proportional to the density of the medium n_0 , the path length L inside the medium and the probability C that a scattering center in the medium interacts with the hard electron. As expected from a particle undergoing random motion in the \mathbf{q}_\perp -plane, the accumulated average \mathbf{q}_\perp^2 grows proportional to L . The corresponding contribution (4.9) is seen explicitly in I_1 and I_6 , but it can also be recovered from I_3 in an expansion to lowest order in α_{em}^2 , when

$$i\mu\Omega \sin(\Omega L) = nCLx^2 + O(\alpha_{\text{em}}^4). \quad (4.10)$$

We now turn to the remaining three contributions of the radiation cross section (4.5), which are given in terms of integrals over the longitudinal extension of the medium:

$$\begin{aligned} I_2^{(\text{osc})} &= \frac{\text{Re}}{Q_1} \int_0^L dz e^{-i\bar{q}z} \frac{\pi x^2}{C_2^2} \times \\ &\left[a_2^{(1)} \mathbf{p}_{1\perp}^2 + a_2^{(12)} \mathbf{p}_{1\perp} \cdot \mathbf{p}_{2\perp} \right] \times \\ &\exp\left\{ \frac{-x^2}{4C_2^2} \left[b_2^{(1)} \mathbf{p}_{1\perp}^2 - 2\mathbf{p}_{1\perp} \cdot \mathbf{p}_{2\perp} + b_2^{(2)} \mathbf{p}_{2\perp}^2 \right] \right\}, \end{aligned} \quad (4.11)$$

$$\begin{aligned} I_5^{(\text{osc})} &= \frac{\text{Re}}{Q_2} \int_0^L dz e^{i\bar{q}(z-L)} \frac{\pi x^2}{C_5^2} \\ &\left[a_5^{(2)} \mathbf{p}_{2\perp}^2 + a_5^{(12)} \mathbf{p}_{1\perp} \cdot \mathbf{p}_{2\perp} \right] \times \\ &\exp\left\{ \frac{-x^2}{4C_5^2} \left[b_5^{(1)} \mathbf{p}_{1\perp}^2 - 2\mathbf{p}_{1\perp} \cdot \mathbf{p}_{2\perp} + b_5^{(2)} \mathbf{p}_{2\perp}^2 \right] \right\}, \end{aligned} \quad (4.12)$$

$$\begin{aligned} I_4^{(\text{osc})} &= -\text{Re} \int_0^L dz \int_z^L dz' e^{-i\bar{q}(z'-z)} \frac{\pi x^2}{C_4^3} \times \\ &\left[a_4^{(0)} + a_4^{(1)} \mathbf{p}_{1\perp}^2 + a_4^{(12)} \mathbf{p}_{1\perp} \cdot \mathbf{p}_{2\perp} + a_4^{(2)} \mathbf{p}_{2\perp}^2 \right] \times \\ &\exp\left\{ \frac{-x^2}{4C_4^3} \left[b_4^{(1)} \mathbf{p}_{1\perp}^2 - 2\mathbf{p}_{1\perp} \cdot \mathbf{p}_{2\perp} + b_4^{(2)} \mathbf{p}_{2\perp}^2 \right] \right\}. \end{aligned} \quad (4.13)$$

To make the structure of these terms transparent, we have introduced several shorthands a_i , b_i and C_i . The factors b_i and C_i show simple limiting behaviour:

$$b_i = 1 + O(\alpha_{\text{em}}^2), \quad (4.14)$$

$$4 C_i = 2 n C L x^2 + O(\alpha_{\text{em}}^4). \quad (4.15)$$

This allows us to recover the Molière \mathbf{q}_\perp -broadening term (4.9) to leading order in the coupling constant in all six contributions $I_j^{(\text{osc})}$ of the radiation spectrum (4.5).

The explicit form of the functions C_i are:

$$C_2 = \frac{i\mu}{2} \Omega \{ \Omega (L - z) \cos[\Omega z] + \sin[\Omega z] \}, \quad (4.16)$$

$$C_5 = \frac{i\mu}{2} \Omega \{ \Omega z \cos[\Omega(L - z)] + \sin[\Omega(L - z)] \}, \quad (4.17)$$

$$C_4 = \frac{i\mu}{2} \Omega \{ -\Omega^2 z (L - z') \sin[\Omega(z' - z)] + \sin[\Omega(z' - z)] \\ + \Omega (L - z' + z) \cos[\Omega(z' - z)] \}, \quad (4.18)$$

from which the limit (4.15) is recovered easily. The functions b_i are given by

$$b_2^{(1)} = \cos[\Omega z] - \Omega (L - z) \sin[\Omega z], \quad (4.19)$$

$$b_2^{(2)} = \cos[\Omega z], \quad (4.20)$$

$$b_5^{(1)} = \cos[\Omega (L - z)], \quad (4.21)$$

$$b_5^{(2)} = \cos[\Omega (L - z)] - \Omega z \sin[\Omega (L - z)], \quad (4.22)$$

$$b_4^{(1)} = \cos[\Omega (z' - z)] - \Omega (L - z') \sin[\Omega (z' - z)], \quad (4.23)$$

$$b_4^{(2)} = \cos[\Omega (z' - z)] - \Omega z \sin[\Omega (z' - z)]. \quad (4.24)$$

from which the limiting form (4.14) is also clear. Finally, the prefactors of the integrands in (4.11)-(4.13) are:

$$a_2^{(1)} = \frac{\mu}{2} \Omega^2 (L - z), \quad a_2^{(12)} = \frac{\mu}{2} \Omega \sin[\Omega z], \quad (4.25)$$

$$a_5^{(2)} = \frac{\mu}{2} \Omega^2 z, \quad a_5^{(12)} = \frac{\mu}{2} \Omega \sin[\Omega (L - z)], \quad (4.26)$$

$$a_4^{(0)} = \mu^2 \Omega^4 C_4 \frac{1}{x^2} z (L - z'), \quad (4.27)$$

$$a_4^{(1)} = \frac{\mu^2 \Omega^4}{4} \left((L - z')^2 c + \frac{L - z'}{\Omega} s \right), \quad (4.28)$$

$$a_4^{(2)} = \frac{\mu^2 \Omega^4}{4} \left(z^2 c + \frac{z}{\Omega} s \right), \quad (4.29)$$

$$a_4^{(12)} = \frac{\mu^2 \Omega^4}{4} \left\{ z(L - z') + \left(z c + \frac{s}{\Omega} \right) \right. \\ \left. \times \left((L - z') c + \frac{s}{\Omega} \right) \right\}, \quad (4.30)$$

where we have used $c \equiv \cos[\Omega(z' - z)]$ and $s \equiv \sin[\Omega(z' - z)]$. The expressions given here allow for a numerical calculation of the radiation spectrum, once the extension L of the medium, its density n_0 , and the measure C of the elastic cross section of a single scatterer are given. Based on these expressions, we discuss in the next subsections i) an analytically accessible limiting case of the spectrum (4.5) and ii) a Bethe-Heitler limit which allows to determine the constant C phenomenologically.

B. Molière limit: Radiation in the Gaussian small angle multiple scattering regime

We now turn to a limiting case of the radiation spectrum (2.22) in which a characteristic in-medium effect can be isolated in a simple analytical expression. This limit focusses on the kinematical region

$$q_\perp \ll k_\perp \ll k \ll E, \quad (4.31)$$

$$Q L = \frac{k_\perp^2}{2k} L \gg 1, \quad (4.32)$$

$$\bar{q} L \gg 1, \quad (4.33)$$

$$|\Omega L| \ll 1. \quad (4.34)$$

The first condition (4.31) is satisfied in the high energy limit when x is small and the photon is radiated under a small angle with respect to the beam. It is characteristic for relativistic kinematics that the transverse momentum freed by multiple interactions can be significantly larger than the total transverse momentum q_\perp transferred by the medium, i.e., $\mathbf{p}_\perp \approx -\mathbf{k}_\perp$ and $q_\perp = |\mathbf{p}_\perp + \mathbf{k}_\perp| \ll k_\perp$. According to (4.32) and (4.33), the length of the medium has to exceed one formation length significantly, while the last condition $|\Omega L| \ll 1$ can be realized e.g. by choosing a target of sufficiently low density. We note that (4.33) is by far the most stringent condition.

As a consequences of (4.32) and (4.33), the terms $\cos(QL)$, $\sin(QL)$ are rapidly oscillating as function of L . If we assume a target with varying extension L , e.g. due to an unpolished surface, then contributions to the radiation spectrum (4.5) proportional to these oscillating terms will be averaged out by the experiment. An expansion of the terms in (4.5) in powers of the coupling constant leads then to

$$I_1^{(\text{osc})} = \frac{1}{2} \frac{\mathbf{p}_{*\perp}^2}{Q^2} \frac{2\pi}{n C L} \exp \left\{ -\frac{\mathbf{q}_\perp^2}{2 n C L} \right\}, \quad (4.35)$$

$$I_2^{(\text{osc})} = \left[\frac{-2\pi}{n C L} \frac{\mathbf{p}_{*\perp}^2}{Q^2} - \frac{4\pi}{Q^2} \frac{1}{L^2 Q^2} \right] e^{-\frac{\mathbf{q}_\perp^2}{2 n C L}}, \quad (4.36)$$

$$I_3^{(\text{osc})} = 0 \quad (4.37)$$

$$I_4^{(\text{osc})} = \left[\frac{2\pi}{n C L} \frac{\mathbf{p}_{*\perp}^2}{Q^2} + \frac{2\pi}{Q^2} + \frac{4\pi}{Q^2} \frac{1}{L^2 Q^2} \right] e^{-\frac{\mathbf{q}_\perp^2}{2 n C L}}, \quad (4.38)$$

$$I_5^{(\text{osc})} = \left[\frac{-2\pi}{n C L} \frac{\mathbf{p}_{*\perp}^2}{Q^2} - \frac{4\pi}{Q^2} \frac{1}{L^2 Q^2} \right] e^{-\frac{\mathbf{q}_\perp^2}{2 n C L}}, \quad (4.39)$$

$$I_6^{(\text{osc})} = \frac{1}{2} \frac{\mathbf{p}_{*\perp}^2}{Q^2} \frac{2\pi}{n C L} \exp \left\{ -\frac{\mathbf{q}_\perp^2}{2 n C L} \right\}. \quad (4.40)$$

Here, we have used (4.32) to neglect the \mathbf{q}_\perp -dependent terms except for the leading $O(1/\alpha_{\text{em}}^2)$ Molière factor (4.9), and we have approximated $\mathbf{p}_{1\perp} \approx \mathbf{p}_{2\perp} \approx \mathbf{p}_{*\perp}$. Corrections to these terms are of order $O(\frac{q_\perp^2}{k_\perp^2})$ and $O(1/(L^2 Q^2)^2)$. Neglecting $O(1/(L^2 Q^2))$ -contributions, the radiation spectrum (4.5) takes the simple form

$$\frac{d^5\sigma}{d(\ln x) d\mathbf{p}_\perp d\mathbf{k}_\perp} = C_{\text{pre}} g_{\text{nf}} \sum_{j=1}^6 I_j^{(\text{osc})} \approx \frac{\alpha_{\text{em}}}{\pi^3} \frac{x^2}{\mathbf{k}_\perp^4} \exp\left\{-\frac{\mathbf{q}_\perp^2}{2nCL}\right\}. \quad (4.41)$$

This Molière limit is the main result of the present subsection. In accordance with the Bethe-Heitler single scattering cross section (3.14), we still find the characteristic x^2 rapidity dependence, as well as the $1/\mathbf{k}_\perp^4$ fall off of the spectrum in the kinematical regime $q_\perp \ll k_\perp$. In contrast to the single scattering Bethe-Heitler cross section, however, the spectrum now peaks at vanishing total momentum transfer $q_\perp = 0$ rather than to vanish for $q_\perp \rightarrow 0$. The reason is that the radiation from many small angle scatterings adds up to a finite contribution, while the sum $\sum_i^N \mathbf{q}_{i\perp}$ of many small random momentum transfers $\mathbf{q}_{i\perp}$ peaks at zero.

Also the dependence of (4.41) on the coupling constant is easy to understand. The cross section is proportional to α_{em} , since one photon is radiated off. The broadening of the \mathbf{q}_\perp -distribution is determined by the probability that the hard electron undergoes an interaction. This probability is given by the elastic single scattering Mott cross section, and hence the exponent shows a characteristic α_{em}^{-2} -dependence.

The radiation cross section (4.5) obtained in the dipole approximation, is clearly more complex than the limiting case (4.41). The latter, however, illustrates most clearly that generic in medium effects are retained in the dipole approximation which cannot be obtained from a calculation to fixed order in the coupling constant.

C. Fixing the dipole parameter C in the Bethe-Heitler limit: validity of the dipole approximation

In the dipole approximation, the expansion of the radiation cross section (2.22) in powers of the coupling constant does not converge. The spectra for $N = 1, 2, 3$ scatterings derived in section III, are proportional to the N -th power of the elastic scattering cross section $\tilde{\Sigma}(\mathbf{q}_\perp)$ which is essentially the Fourier transform of $\sigma(\boldsymbol{\rho})$. While the Fourier transform of the analytic expression (A11) for $\sigma(\boldsymbol{\rho})$ is well-defined, the Fourier transform of its dipole approximation $\sigma(\boldsymbol{\rho}) = C \boldsymbol{\rho}^2$ diverges.

This failure of the dipole approximation to allow for an expansion of (2.22) in powers of the opacity \mathcal{T} does not affect its validity for the calculation of medium effects as given e.g. in the last subsections. This can be seen e.g. from the factor $\exp\{-\int \Sigma(\xi, x \boldsymbol{\rho})\}$ in (2.22). Its Fourier transform is well-defined and it is well approximated in the dipole approximation $\sigma(\boldsymbol{\rho}) = C \boldsymbol{\rho}^2$ by a Gaussian of appropriate width. It is only the expansion of this factor in α_{em} whose Fourier transform does not receive the main

contributions from small values around $\rho = 0$. This is the reason why the dipole approximation of $\sigma(\boldsymbol{\rho})$ for small values of $\boldsymbol{\rho}$ cannot be combined without difficulties with an expansion in the coupling constant.

For the \mathbf{q}_\perp -integrated spectrum (2.47), this technical difficulty does not exist. The reason is that in the integrand of (2.47), the first order term $\Sigma(\xi, x \boldsymbol{\rho}_1)$ comes multiplied by $\mathcal{K}(z', 0; z, \boldsymbol{\rho}_1 | \mu)$ which is to lowest order in the coupling constant a Gaussian in $\boldsymbol{\rho}_1$. This ensures that the main contribution to the integral (2.47) comes from small values of $\boldsymbol{\rho}$ where the dipole approximation is valid. The corresponding Bethe-Heitler spectrum in which the dipole approximation is employed *after* integrating out the \mathbf{q}_\perp -dependence, reads:

$$\frac{d^3\sigma}{d(\ln x) d\mathbf{k}_\perp} \Big|_{O(\alpha_{\text{em}}^3 \mathcal{T})}^{\text{dipole}} = \frac{\alpha_{\text{em}}}{2\pi^2} x^2 C \{4 - 4x + 2x^2\} \times \frac{\mathbf{k}_\perp^4 + (m_e x)^4}{(\mathbf{k}_\perp^2 + (m_e x)^2)^4} \mathcal{T}. \quad (4.42)$$

In the calculation of (4.42) we have not neglected the \bar{q} -dependence of the radiation spectrum (2.22). The consequence is the appearance of the very small term $m_e x$ which regulates the $\frac{1}{\mathbf{k}_\perp^4}$ singularity. This allows to calculate the \mathbf{k}_\perp -integrated Bethe-Heitler energy loss formula in the dipole approximation

$$\frac{d\sigma}{d(\ln x)} \Big|_{O(\alpha_{\text{em}}^3 n)}^{\text{dipole}} = \frac{\alpha_{\text{em}} C}{3\pi m_e^2} \{4 - 4x + 2x^2\} \times \left(1 - m_e^2 x^2 \frac{3\omega^4 + 3\omega^2 m_e^2 x^2 + m_e^4 x^4}{2(\omega^2 + m_e^2 x^2)^3}\right). \quad (4.43)$$

We note that except for the small correction from the kinematical boundary $\omega = E_1 x$ of the \mathbf{k}_\perp -integral, expression (4.43) is consistent with the Bethe-Heitler term derived by Zakharov in the dipole approximation [17]. Equations (4.42) or (4.43) allow to determine the only free parameter C from a comparison with well-tabulated Bethe-Heitler scattering cross section [35]. Once, C is fixed, the radiation spectrum (4.5) in the dipole approximation provides thus a parameter free prediction of the measured in-medium energy loss. Zakharov has pursued this strategy to fix C in his \mathbf{q}_\perp - and \mathbf{k}_\perp -integrated spectrum (2.49), and this has lead to a very successful description of the SLAC-146 data on radiative energy loss [17].

V. THE DIPOLE PRESCRIPTION FOR QCD

To calculate the integrated QCD radiative energy loss of a hard coloured parton, Zakharov [17] has used a very simple substitution in his energy loss formula (2.49). This QCD dipole prescription consists in replacing the

dipole cross section $\sigma(x\boldsymbol{\rho})$ in the calculation of the QED radiation spectrum by a combination of three dipole cross sections [30]:

$$\sigma_{\text{QED}}(\boldsymbol{\rho}, x) = \sigma(x\boldsymbol{\rho}) \longrightarrow \sigma_{\text{QCD}}(\boldsymbol{\rho}, x) = \frac{9}{8} \{ \bar{\sigma}(\boldsymbol{\rho}) + \bar{\sigma}((1-x)\boldsymbol{\rho}) \} - \frac{1}{8} \bar{\sigma}(x\boldsymbol{\rho}). \quad (5.1)$$

Here, we have chosen $\bar{\sigma}$ proportional to the elastic q - q Mott cross section, cf. subsection V A. The heuristic argument for the prescription (5.1) starts from the representation of the projectile quark in the light cone frame as a superposition of the bare quark and higher Fock states,

$$|\text{projectile}\rangle = |q\rangle + |q\gamma\rangle + \dots \quad (5.2)$$

If all Fock components interact with the external potentials with the same amplitude, then the coherence between these amplitudes is not disturbed, and no bremsstrahlung is generated. The radiation amplitude depends hence on the difference between the elastic scattering amplitudes of different fluctuations. The dipole cross section $\sigma(x\boldsymbol{\rho})$ contains information about this difference since it arises from averaging in (2.20) the (part of the) amplitude M_{fi} for the "ingoing" $|q\rangle$ with the (part of the) complex conjugated amplitude M_{fi}^* for the "outgoing" higher Fock state $|q\gamma\rangle$. In the transverse plane, the separation of the $|q\gamma\rangle$ fluctuation from the ingoing q can be estimated via the uncertainty relation: $x_{\perp}\gamma \propto \frac{k_{\perp}}{x E_1} \frac{1}{\Delta E} \propto (1-x)/k_{\perp}$ and $x_{\perp}q \propto \frac{k_{\perp}}{(1-x) E_1} \frac{1}{\Delta E} \propto x/k_{\perp}$. The transverse distance $\boldsymbol{\rho}$ is linked to the transverse momentum in (2.22) by a Fourier transform and we may think of $\boldsymbol{\rho}$ as the transverse size of the \bar{q} - γ fluctuation. With the transverse center of mass of this fluctuation at the position of the ingoing quark $|q\rangle$, see Figure 2, the transverse distance between the charged components q and \bar{q} is then $x\boldsymbol{\rho}$, and it is the dipole of this size which determines the radiation spectrum. For related arguments, see also Ref. [33].

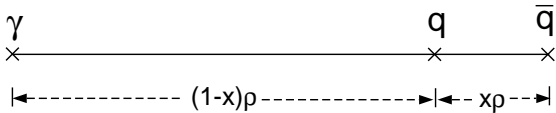


FIG. 2. Separation of dipoles in the transverse plane: the \bar{q} - γ fluctuation of transverse size ρ gives rise to a QED radiation spectrum determined by the \bar{q} - q dipole of size $x\rho$. In QCD, where the radiated gluon is charged, all three dipole contributions should be considered. More details are given in (5.1) and the following text.

In QCD, the emitted gluon is charged too, and aside from the q - \bar{q} dipole of size $x\boldsymbol{\rho}$, there is a g - \bar{q} dipole of size $\boldsymbol{\rho}$ and a g - q dipole of size $(1-x)\boldsymbol{\rho}$. The prefactors introduced for these dipoles in the prescription (5.1) stem from interpolating between the limits

$$\lim_{x \rightarrow 0} \sigma_{\text{QCD}}(\boldsymbol{\rho}, x) = \frac{9}{4} \bar{\sigma}(\boldsymbol{\rho}), \quad (5.3)$$

$$\lim_{x \rightarrow 1} \sigma_{\text{QCD}}(\boldsymbol{\rho}, x) = \bar{\sigma}(\boldsymbol{\rho}). \quad (5.4)$$

In the limit $x \rightarrow 0$, the $q\bar{q}$ pair is indistinguishable from a pointlike color-octet charge and the ratio 9/4 of the octet to triplet couplings arises. In the opposite limit $x \rightarrow 1$, the gluon-quark pair at vanishing separation is indistinguishable from a pointlike quark.

The question to what extent this intuitive physical picture leads to the correct QCD radiation cross section was addressed recently in Ref. [26]. There it is argued that Zakharov's integrated energy loss formula (2.49) coincides for QCD with the result of their calculation based on time-ordered perturbation theory. For a discussion of the terms neglected in this approach, see Ref. [34]. Here, we contribute to this discussion by comparing the transverse momentum dependence resulting from the QCD dipole prescription (5.1) to the transverse momentum dependent radiation cross sections for $N = 1$ and $N = 2$ scattering centers, calculated [34] in time-ordered perturbation theory.

A. The Bertsch-Gunion spectrum for $N = 1$ in the QCD dipole prescription

In the present subsection, we test the QCD dipole prescription (5.1) for the case of $N = 1$ scattering. We start from the $N = 1$ QED Bethe-Heitler spectrum (3.14) in the form

$$\frac{d^5 \sigma^{\text{BH-QED}}}{d(\ln x) d\mathbf{q}_{\perp} d\mathbf{k}_{\perp}} = \frac{4 \alpha_{\text{em}}}{(2\pi)^2} \frac{x^2 \mathbf{q}_{\perp}^2}{\mathbf{k}_{\perp}^2 (\mathbf{k}_{\perp} - x \mathbf{q}_{\perp})^2} \mathcal{T} \times \frac{-1}{2} \int \frac{d(x\boldsymbol{\rho})}{(2\pi)^2} \sigma_{\text{QED}}(x\boldsymbol{\rho}) \exp\{i x \mathbf{q}_{\perp} \cdot \boldsymbol{\rho}\}. \quad (5.5)$$

To specify the absolute size of $\bar{\sigma}$ in (5.1), we relate the elastic QED e^-e^- cross section to the corresponding QCD one by

$$\begin{aligned} \frac{-1}{2} \int \frac{d\mathbf{r}}{(2\pi)^2} \sigma(\mathbf{r}) e^{i \mathbf{q}_{\perp} \cdot \mathbf{r}} &= \frac{4 Z^2 \alpha_{\text{em}}^2}{(M^2 + \mathbf{q}_{\perp}^2)^2} \\ \longrightarrow \frac{-1}{2} \int \frac{d\mathbf{r}}{(2\pi)^2} \bar{\sigma}(\mathbf{r}) e^{i \mathbf{q}_{\perp} \cdot \mathbf{r}} &= C_i \frac{4 \alpha_s^2}{(M^2 + \mathbf{q}_{\perp}^2)^2}, \end{aligned} \quad (5.6)$$

where C_i denotes the colour factor, $2 C_i = \frac{4}{9}, 1, \frac{9}{4}$, for q - q , q - g , g - g . Also, to change to the QCD-case, we replace the coupling to the emitted photon in (5.5) by $\alpha_{\text{em}} \rightarrow \alpha_s C_A$, where the Casimir C_A of the adjoint representation accounts for the emitted gluon. With this input, we follow the dipole prescription and substitute (5.1) in the Bethe-Heitler cross section (5.5). After rescaling $\mathbf{q}_{\perp} \rightarrow \frac{1}{x} \mathbf{q}_{\perp}$ on both sides of the equation, we find (note that $\bar{\sigma}(x\boldsymbol{\rho}) = \bar{\sigma}((1-x)\boldsymbol{\rho}) + O(x)$)

$$\frac{d^5 \sigma^{\text{BG-QCD}}}{d(\ln x) d\mathbf{q}_\perp d\mathbf{k}_\perp} = \frac{C_A \alpha_s}{\pi^2} \frac{\mathbf{q}_\perp^2}{\mathbf{k}_\perp^2 (\mathbf{k}_\perp - \mathbf{q}_\perp)^2} \mathcal{T} \times \frac{8}{9} \frac{\alpha_s^2}{(M^2 + \mathbf{q}_\perp^2)^2} + O(x). \quad (5.7)$$

This is the Bertsch-Gunion radiation spectrum [36] times the elastic Mott cross section for a Debye-screened coloured potential. For $N = 1$, the QCD dipole prescription turns to leading order $O(1/E)$ the Bethe-Heitler QED radiation spectrum *exactly* into the Bertsch-Gunion QCD radiation spectrum. This success does not depend on the particular combination of colour dipoles introduced in (5.1). It is rather due to the scaling property of the dipole size in (5.5): replacing in the argument of σ the transverse extension $x \boldsymbol{\rho} \rightarrow \boldsymbol{\rho}$ modifies both: (i) the x^2 rapidity distribution of the QED spectrum into the flat rapidity distribution of the QCD spectrum and (ii) the characteristic $x \mathbf{q}_\perp$ -dependence of the QED spectrum into the characteristic \mathbf{q}_\perp -dependence of the QCD radiation spectrum.

B. Corrections to the QCD dipole prescription for $N = 2$

The interference terms of QCD multiple scattering bremsstrahlung radiation are more complicated than their QED analogue. Especially, since the gluon is charged, it can rescatter on additional potentials, and these cascading contributions do not factorize from the gluon production amplitudes. This effect does not exist for the QED bremsstrahlung: there, the only in medium modification of the produced photons is the dielectric suppression which is clearly a final state effect which factorizes from the production amplitude.

This qualitatively different structure of QCD rescattering processes makes it interesting to study the accuracy of the QCD dipole prescription for $N = 2$ scatterings. To this aim, we compare the $N = 2$ radiation spectrum (3.15) to the result of the full $N = 2$ QCD radiation spectrum calculated in time ordered perturbation theory in Ref. [34]:

$$\begin{aligned} \frac{d^5 \sigma_{N=2}^{\text{full QCD}}}{d(\ln x) d\mathbf{q}_\perp d\mathbf{k}_\perp} &= \frac{C_A \alpha_s}{\pi^2} \int d\mathcal{V}_{\text{QCD}}^2(\mathbf{q}_\perp) \\ &\times \left\{ \vec{B}_1^2 + \vec{B}_2^2 + R \vec{B}_{2(12)}^2 - \frac{C_A}{2C_F} \left(\vec{B}_1 \cdot \vec{B}_2 \cos(\omega_1 \Delta t) \right. \right. \\ &\quad \left. \left. - 2 \vec{B}_2 \cdot \vec{B}_{2(12)} \cos(\omega_2 \Delta t) \right. \right. \\ &\quad \left. \left. + \vec{B}_1 \cdot \vec{B}_{2(12)} \cos(\omega_{20} \Delta t) \right) \right\}, \end{aligned} \quad (5.8)$$

where $\omega_0 = \frac{\mathbf{k}_\perp^2}{2\omega}$, $\omega_2 = \frac{(\mathbf{k}_\perp - \mathbf{q}_{2\perp})^2}{2\omega}$, $\omega_{20} = \omega_2 - \omega_0$. Equation (5.8) is obtained by squaring the amplitude in Eq. (2.20) of Ref. [23] which corresponds to the seven diagrams in Fig. 3. We have used the following shorthands:

$$\begin{aligned} \int d\mathcal{V}_{\text{QCD}}^2(\mathbf{q}_\perp) &= \int d\mathbf{q}_{1\perp} d\mathbf{q}_{2\perp} \frac{\frac{8}{9} \alpha_s^2}{(M^2 + \mathbf{q}_{1\perp}^2)^2} \\ &\times \frac{\frac{8}{9} \alpha_s^2}{(M^2 + \mathbf{q}_{2\perp}^2)^2} \delta^{(2)}(\mathbf{q}_\perp - \mathbf{q}_{1\perp} - \mathbf{q}_{2\perp}), \end{aligned} \quad (5.9)$$

$$\vec{B}_i = \frac{\mathbf{k}_\perp}{\mathbf{k}_\perp^2} - \frac{\mathbf{k}_\perp - \mathbf{q}_{i\perp}}{(\mathbf{k}_\perp - \mathbf{q}_{i\perp})^2}, \quad (5.10)$$

$$\vec{B}_{i(12)} = \frac{\mathbf{k}_\perp - \mathbf{q}_{i\perp}}{(\mathbf{k}_\perp - \mathbf{q}_{i\perp})^2} - \frac{\mathbf{k}_\perp - \mathbf{q}_{1\perp} - \mathbf{q}_{2\perp}}{(\mathbf{k}_\perp - \mathbf{q}_{1\perp} - \mathbf{q}_{2\perp})^2}. \quad (5.11)$$

The $N = 2$ radiation spectrum (5.8) is obtained for the case of two scattering centers placed at *fixed* longitudinal positions $z_1 = t_1$, $z_2 = t_2$ with $\Delta t = t_2 - t_1$. In contrast, the $N = 2$ calculation presented in section IIIB considers two scattering centers at *arbitrary* longitudinal positions distributed according to a homogeneous density n_0 within a longitudinal extension L . In fact, the interference terms in (5.8) depend in a different way on the kinematical variables than the interference terms in (3.16). Moreover, we cannot compare the $\Delta t \rightarrow 0$ limit of both expressions, since (5.8) is obtained in time ordered perturbation theory where $t_1 < t_2$ is used to neglect diagrammatic contributions. This leaves us for a direct comparison of both calculations with only the limiting case

$$\begin{aligned} \lim_{\Delta t \rightarrow \infty} \frac{d^5 \sigma_{N=2}^{\text{full QCD}}}{d(\ln x) d\mathbf{q}_\perp d\mathbf{k}_\perp} &= \frac{C_A \alpha_s}{\pi^2} \int d\mathcal{V}_{\text{QCD}}^2(\mathbf{q}_\perp) \\ &\times \left\{ \vec{B}_1^2 + \vec{B}_2^2 + \frac{C_A}{C_F} \vec{B}_{2(12)}^2 \right\}, \end{aligned} \quad (5.12)$$

which corresponds to two scattering centers at arbitrary large relative distance. One checks that the QCD dipole prescription leads for the $N = 2$ rescattering result (3.26) in the $L \rightarrow \infty$ limit

$$\begin{aligned} \lim_{L \rightarrow \infty} \frac{d^5 \sigma_{N=2}^{\text{dipole QCD}}}{d(\ln x) d\mathbf{q}_\perp d\mathbf{k}_\perp} &= \frac{C_A \alpha_s}{\pi^2} \int d\mathcal{V}_{\text{QCD}}^2(\mathbf{q}_\perp) \\ &\times \left\{ \vec{B}_1^2 + \vec{B}_{1(12)}^2 \right\} \frac{\mathcal{T}^2}{2}. \end{aligned} \quad (5.13)$$

Due to the symmetry of the $\mathbf{q}_{1\perp}$ - and $\mathbf{q}_{2\perp}$ -integrations, one can exchange $\vec{B}_{1(12)}^2 \rightarrow \vec{B}_{2(12)}^2$ in (5.13). Also, for a direct comparison with the $N = 2$ case (5.12), the opacity factor $\frac{\mathcal{T}^2}{2}$ that corresponds to the probability of two scatterings, should be dropped.

To discuss the differences between the result (5.13) of the QCD dipole prescription and the $N = 2$ pQCD result (5.12), we present in Figure 3 the seven Feynman amplitudes contributing to the radiation spectrum (5.8). For each of the diagrams, we denote by M_i the entire contribution, by $M_i^{(1)}$ the part of the contribution whose phase factor depends only on t_1 , by $M_i^{(12)}$ the part whose phase factor depends on t_1 and t_2 , etc. Based on calculations reported in Ref. [23, 34], one finds

$$\vec{B}_1^2 \propto (M_1 + M_2^{(1)} + M_4)^2, \quad (5.14)$$

$$\vec{B}_2^2 \propto (M_2^{(2)} + M_3 + M_6^{(2)})^2, \quad (5.15)$$

$$\vec{B}_{2(12)}^2 \propto (M_5 + M_6^{(12)} + M_7)^2. \quad (5.16)$$

As can be seen from Figure 3, the terms \vec{B}_1^2 and \vec{B}_2^2 are the Bertsch-Gunion radiation contributions off the first and second scattering center respectively. The term $\vec{B}_{2(12)}^2$ corresponds to gluon emission around t_1 and rescattering of the gluon at t_2 . Since it is the gluon and not the quark which scatters off the second coloured potential, the term $\vec{B}_{2(12)}^2$ is enhanced by a factor $\frac{C_A}{C_F}$ in (5.12). These three sets of diagrams leading to \vec{B}_1^2 , \vec{B}_2^2 and $\vec{B}_{2(12)}^2$ can also be seen to form the building blocks of an effective current in the BDMPS-approach, see e.g. Fig. 4 of Ref. [23].

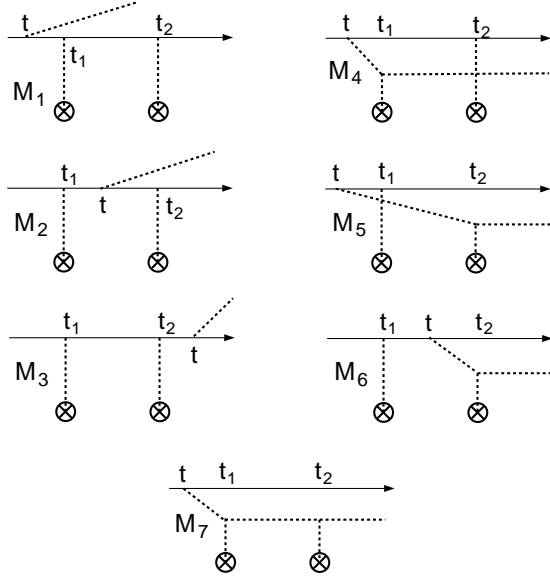


FIG. 3. The seven contributions to the $N = 2$ QCD radiation spectrum in time-ordered perturbation theory. In the large distance limit, the Bertsch-Gunion and gluon cascading contributions can be identified with particular combinations of these diagrams, see equations (5.14) - (5.16) and the text.

One might have expected naively that the QCD dipole prescription maps the two Bethe-Heitler terms of (3.26) onto the two Bertsch-Gunion terms \vec{B}_1^2 and \vec{B}_2^2 . This is only the case for the \mathbf{k}_\perp -integrated cross section (i.e., the energy loss) if the kinematical boundary $\omega = x E_1$ is ignored. Then, the \mathbf{k}_\perp -integration allows to shift $\mathbf{k}_\perp \rightarrow \mathbf{k}_\perp - \mathbf{q}_{1\perp}$ which changes $\vec{B}_{1(12)}^2 \rightarrow \vec{B}_2^2$ in (5.13).

The $N = 2$ low opacity expansion allows a quantitative check of QED-inspired QCD calculations. The deviation of the limiting case (5.13) from the perturbative QCD result is clearly non-negligible: for the \mathbf{k}_\perp -integrated case, where the $\vec{B}_{1(12)}^2$ and \vec{B}_1^2 -contributions have the same size, one can read off a correction factor

$$F_{\text{corr}} = 1 + \frac{C_A}{2 C_F} = \frac{17}{8}, \quad (5.17)$$

with which the $N = 2$ dipole cross section (5.13) has to be multiplied to regain the pQCD radiation spectrum. [In fact, for QCD, the \mathbf{k}_\perp -integrals are divergent in the $\Delta t \rightarrow \infty$ limit due to the collinear singularity that must be regulated by an in-medium screening scale.] For the \mathbf{k}_\perp - differential spectrum or for finite L , corrections are clearly more complicated, but the important message is that at least for simple few-rescattering cases, the resulting expressions can be compared to pQCD results and the deviations can be quantified. The fact that the QCD dipole prescription tends to underestimate the full pQCD radiation cross section by a significant amount (at least for $N = 2$) may indicate that it is of use as a lower bound for the possible radiative energy loss.

VI. CONCLUSION

In the present work, we have extended the KST-formalism [27] for quantum electrodynamics in several ways: (i) We have supplemented it with a regularization prescription which correctly removes the Weizsäcker-Williams fields of the asymptotic states from the radiation spectrum and thus warrants the correct limiting behaviour of the formalism for a set of few-scattering scenarios. (ii) We have calculated the corresponding angular integrated energy loss and shown that it implies corrections to Zakharov's energy loss formula (2.49). (iii) We have derived a properly regularized radiation spectrum in the dipole approximation which allows for a straightforward numerical calculation, as well as for further analytical studies in limiting cases. Most importantly, the KST-formalism describes the angular dependence of the radiative energy loss which was shown in section IV to have a very rich non-analytical structure, incorporating intuitive properties of in-medium propagation as e.g. the Molière \mathbf{q}_\perp -broadening.

In the QCD case, the situation is much more complex due to the colour structure and the rescattering of the gluon. We have tested the QCD dipole prescription, used in various previous applications [15, 17, 27, 28, 30], against few-scattering pQCD results [34]. The good news is that this prescription recovers the $N = 1$ QCD Bertsch-Gunion gluon radiation spectrum. For multiple collisions, however, even the angular integrated distributions differ from the exact result by a sizeable factor which approaches 17/8 at large separation. This discrepancy is due to the increase in the effective elastic cross section because both the jet and the gluon undergo multiple scattering. Clearly, the QCD problem still needs further work and the present formalism needs to be extended to properly take into account non-abelian features. The introduction of the low opacity expansion in this paper

was shown to be a powerful test of any proposed extension of QED calculations to QCD.

ACKNOWLEDGMENTS

We thank Boris Kopeliovich and Andreas Schäfer for several discussions, especially about the problem of regaining the Bethe-Heitler limit from the radiation spectrum of Ref. [27]. After informing them about the importance of the regularization prescription discussed in section IIB, Boris Kopeliovich noted that Alexander Tarasov had come to the same conclusion on the basis of earlier calculations of one of us. We also thank Peter Levai and Ivan Vitev for many discussions about radiative energy loss calculations in the BDMPs-formalism and for sharing with us the unpublished result (5.8) whose derivation will appear in [34]. Finally, we thank U. Heinz for helpful comments regarding the manuscript. This work was supported by the Director, Office of Energy Research, Division of Nuclear Physics of the Office of High Energy and Nuclear Physics of the U.S. Department of Energy under Contract No. De-FG-02-92ER-40764.

APPENDIX A: IN MEDIUM AVERAGES

In this appendix, we give details of the calculation of in medium averages, used in the derivation of the radiation probability (2.22). We start from a set of N static external potentials U_0 at positions (\mathbf{r}_i, z_i) ,

$$U(\mathbf{x}) = \sum_{i=1}^N U_0(\mathbf{r} - \mathbf{r}_i, \xi - z_i). \quad (\text{A1})$$

The in medium average $\langle \dots \rangle$ averages over the elementary scattering centers in a volume of longitudinal extension Δz and transverse radius R according to

$$\begin{aligned} \langle f \rangle &\equiv \left(\prod_{i=1}^N \int_V \frac{dz_i d\mathbf{r}_i}{\pi R^2 \Delta z} \right) f(\mathbf{r}_1, \dots, \mathbf{r}_N; z_1, \dots, z_N), \\ \langle 1 \rangle &= 1. \end{aligned} \quad (\text{A2})$$

We are interested in the combinations \mathcal{F} of external potentials appearing in the squared radiation amplitude (2.18),

$$\mathcal{F}[\mathbf{r} - \mathbf{r}'; z', z] = \left\langle \exp \left\{ \sum_{i=1}^N W_i(\mathbf{r}, \mathbf{r}'; z', z) \right\} \right\rangle, \quad (\text{A3})$$

$$\begin{aligned} W_i(\mathbf{r}, \mathbf{r}'; z', z) = \\ i \int_z^{z'} d\xi [U(\mathbf{r} - \mathbf{r}_i, \xi - z_i) - U(\mathbf{r}' - \mathbf{r}_i, \xi - z_i)]. \end{aligned} \quad (\text{A4})$$

With a density $n(z_i, \mathbf{r}_i)$ of scattering centers (which is $n = N/\pi R^2 \Delta z$ for the homogeneous case), the average (A3) can be rewritten in the form

$$\begin{aligned} \left\langle \exp \left\{ \sum_{i=1}^N W_i \right\} \right\rangle &= \prod_{i=1}^N \langle e^{W_i} \rangle \\ &= \left(\frac{1}{N} \int dz_i d\mathbf{r}_i n(z_i, \mathbf{r}_i) e^{W_i} \right)^N \\ &\equiv \left(1 + \frac{\bar{\Sigma}}{N} \right)^N \longrightarrow e^{\bar{\Sigma}} \\ &\quad (\text{for } N \rightarrow \infty), \end{aligned} \quad (\text{A5})$$

$$\bar{\Sigma} = \int dz_i d\mathbf{r}_i n(z_i, \mathbf{r}_i) \left(e^{W_i(\mathbf{r}, \mathbf{r}'; z', z)} - 1 \right). \quad (\text{A6})$$

The notational shorthand $\bar{\Sigma}$ introduced here does *not* grow linearly with the number of scattering centers N . This is crucial for the $N \rightarrow \infty$ limit in (A5) to work.

So far, we have not specified the remaining functional dependence of $\bar{\Sigma}$ in (A6). For homogeneous targets of sufficiently large transverse size, it is clear that $\bar{\Sigma}$ can only depend on the relative path difference $\boldsymbol{\rho}(\xi) = \mathbf{r}(\xi) - \mathbf{r}'(\xi)$. We now demonstrate for a specific model that $\bar{\Sigma}$ takes the form

$$\bar{\Sigma}[\boldsymbol{\rho}] = - \int_z^{z'} d\xi \Sigma(\xi, \boldsymbol{\rho}(\xi)), \quad (\text{A7})$$

where $\Sigma(\xi, \boldsymbol{\rho}(\xi)) = \frac{1}{2} n(\xi) \sigma(\boldsymbol{\rho}(\xi))$ is defined in terms of the so-called dipole cross section $\sigma(\boldsymbol{\rho})$ and the longitudinal density $n(\xi)$ of scattering centers, see (2.21).

The model under consideration is the abelian version of the Gyulassy-Wang model which takes for the elementary scattering centers in (A1) Yukawa potentials with Debye mass M ,

$$U_0(\mathbf{x}) = \frac{Z e^2 e^{-M|\mathbf{x}|}}{4\pi |\mathbf{x}|}. \quad (\text{A8})$$

We have included in the definition of these potentials an extra power in the coupling constant to take the coupling of the potential to the passing electron into account. In the following calculation, we assume that the average range $1/M$ of the potentials U_0 is much smaller than the size of the medium, $z' - z \gg 1/M$. Also, we use that density fluctuations are negligible on the scale $1/M$. Expanding $\bar{\Sigma}$ to leading non-vanishing order in the coupling constant e , we find

$$\begin{aligned} \sigma(\boldsymbol{\rho}(\xi)) &= 2 \int_{-\infty}^{\infty} d\xi [\langle U_0(\mathbf{0}, 0) U_0(\mathbf{0}, \xi') \rangle \\ &\quad - \langle U_0(\mathbf{0}, 0) U_0(\boldsymbol{\rho}(\xi), \xi') \rangle], \end{aligned} \quad (\text{A9})$$

where

$$\langle\langle U_0(0) U_0(\mathbf{x}) \rangle\rangle \equiv \int d\bar{\mathbf{x}} U_0(\bar{\mathbf{x}}) U_0(\bar{\mathbf{x}} - \mathbf{x}). \quad (\text{A10})$$

The integrals in (A9) can be done analytically, leading to Zakharov's result [32]

$$\sigma(\rho) = \frac{Z^2 \alpha_{\text{em}}^2}{M^2} 8\pi (1 - M\rho K_1(M\rho)). \quad (\text{A11})$$

In our study of the \mathbf{k}_\perp -dependence of the radiation probability, we shall encounter the Fourier transform of $\tilde{\Sigma}[\rho]$ with respect to the transverse momentum transfer \mathbf{q}_\perp from the medium to the electron,

$$\begin{aligned} \tilde{\Sigma}(\mathbf{q}_\perp) &= \frac{1}{2} \int \frac{d\rho}{(2\pi)^2} \sigma(\rho) \exp\{i\mathbf{q}_\perp \cdot \rho\} \\ &= -\frac{4Z^2 \alpha_{\text{em}}^2}{(M^2 + \mathbf{q}_\perp^2)^2} + \frac{4\pi Z^2 \alpha_{\text{em}}^2}{M^2} \delta^{(2)}(\mathbf{q}_\perp). \end{aligned} \quad (\text{A12})$$

For non-vanishing momentum transfer, the first term of (A12) is the Mott cross-section for electron scattering off the single external potential (A1) in the relativistic limit. The size of the prefactor of the $\delta^{(2)}(\mathbf{q}_\perp)$ contribution is such that the \mathbf{q}_\perp -integral over (A12) vanishes. This warrants that the dipole cross section $\sigma(\rho)$ vanishes at vanishing dipole size $\rho = 0$. One can trace back the origin of this second term: in the expansion of (A4) to second order in the coupling constant, it arises from contributions which are second order in $U(\mathbf{r} - \mathbf{r}_i)$ but zeroth order in $U(\mathbf{r}' - \mathbf{r}_i)$, or vice versa. This amounts to multiplying the second order term of $M_{fi}^{(2)}$ with the zeroth order term $M_{fi}^{(0)*}$ of the complex conjugated amplitude. The contribution $M_{fi}^{(2)} \times M_{fi}^{(0)*}$ to the radiation cross section vanishes however due to energy momentum conservation. Calculating such a contribution from the Furry approximation (2.5), (2.6), this energy momentum conservation appears in the form of a $\delta^{(2)}(\mathbf{q}_\perp)$, resulting in an additional contribution to the Mott cross section. For a comparison with experimental data, one has to assume a transverse momentum transfer \mathbf{q}_\perp which is always finite but can become arbitrarily small. Then the second term in (A12) drops out in all physical quantities.

APPENDIX B: EIKONAL EXPRESSIONS FROM PATH INTEGRALS

In this appendix, we give details of the solutions of the path integrals, used for the derivation of the radiation probability $\langle|M_{fi}|^2\rangle$ in (2.22). We start from the observation that with the help of the averaging (2.20)

$$\begin{aligned} &\mathcal{S}(z', \mathbf{r}(z'), \mathbf{r}'(z'); z, \mathbf{r}(z), \mathbf{r}'(z)|p) \\ &\equiv \langle G(z', \mathbf{r}(z'); z, \mathbf{r}(z)|p) G^*(z', \mathbf{r}'(z'); z, \mathbf{r}'(z)|p) \rangle \\ &= \int \mathcal{D}\bar{\rho} \mathcal{D}\hat{\rho} \exp \left\{ \frac{ip}{2} \int_z^{z'} \dot{\hat{\rho}} \cdot \dot{\bar{\rho}} \right\} \mathcal{F}[\hat{\rho}; z', z], \end{aligned} \quad (\text{B1})$$

$$\hat{\rho}(z) = \mathbf{r}(z) - \mathbf{r}'(z), \quad \bar{\rho}(z) = \mathbf{r}(z) + \mathbf{r}'(z). \quad (\text{B2})$$

Here, the dot denotes a derivative with respect to the longitudinal direction and the integral $\int \mathcal{D}\bar{\rho}$ is trivial. It results in a δ -function which constrains all possible paths $\hat{\rho}(\xi)$ by the mid-point rule to a straight line

$$\hat{\rho}_s(\xi) = \hat{\rho}(z') \frac{\xi - z}{z' - z} + \hat{\rho}(z) \frac{z' - \xi}{z' - z}. \quad (\text{B3})$$

The final result is

$$\begin{aligned} &\mathcal{S}(z', \mathbf{r}(z'), \mathbf{r}'(z'); z, \mathbf{r}(z), \mathbf{r}'(z)|p) \\ &= - \left(\frac{p}{2\pi i(z' - z)} \right)^2 \exp \left\{ - \int_z^{z'} \Sigma(\xi, \hat{\rho}_s(\xi)) d\xi \right\} \\ &\times \exp \left\{ \frac{ip \left[(\mathbf{r}(z') - \mathbf{r}(z))^2 - (\mathbf{r}'(z') - \mathbf{r}'(z))^2 \right]}{2(z' - z)} \right\}, \end{aligned} \quad (\text{B4})$$

We note that this 'eikonal path' $\hat{\rho}_s$ does not result from an eikonal approximation. It is rather obtained from a calculation on the cross section level, once the ingoing and outgoing states Ψ_F^\pm of (2.5), (2.6) are adopted as starting point: the Furry approximation is a systematic expansion in $1/E$ and thus closely related to the eikonal approximation.

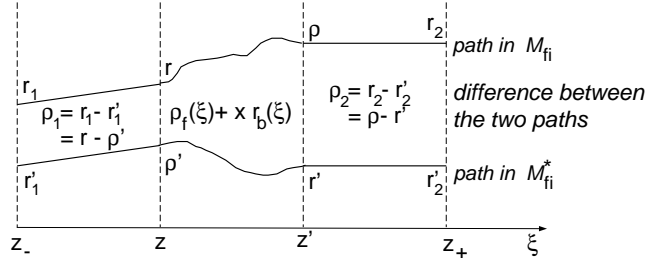


FIG. 4. Diagrammatic representation of the path integrals appearing in the radiation probability (2.22). According to (B1), the path differences ρ_1 and ρ_2 at early times $\xi < z$ and late times $\xi > z'$ are fixed to straight lines. Between z and z' , the path difference can change due to interactions with the medium, but the boundary conditions are fixed.

The explicit expression (B4) allows to simplify the radiation probability (2.18) by using

$$\begin{aligned} &\int d\mathbf{r}_2 d\mathbf{r}'_2 e^{-i\mathbf{p}_{2\perp} \cdot (\mathbf{r}_2 - \mathbf{r}'_2)} S(z_+, \mathbf{r}_2, \mathbf{r}'_2; z', \rho, \mathbf{r}'|p_2) \\ &= - \exp \left\{ -i\mathbf{p}_{2\perp} \cdot \rho_2 - \int_{z'}^{z_+} \Sigma(\xi, \rho_2) d\xi \right\}, \end{aligned} \quad (\text{B5})$$

$$\begin{aligned} &\int d\mathbf{r}_1 d\mathbf{r}'_1 e^{i\mathbf{p}_{1\perp} \cdot (\mathbf{r}_1 - \mathbf{r}'_1)} S(z, \mathbf{r}, \mathbf{r}'; z_-, \mathbf{r}_1, \mathbf{r}'_1|p_1) \\ &= - \exp \left\{ i\mathbf{p}_{1\perp} \cdot \rho_1 - \int_{z_-}^z \Sigma(\xi, \rho_1) d\xi \right\}, \end{aligned} \quad (\text{B6})$$

where we have introduced the coordinates

$$\begin{aligned} \rho_1 &= \mathbf{r} - \rho', & \bar{\rho}_1 &= \mathbf{r} + \rho', \\ \rho_2 &= \rho - \mathbf{r}', & \bar{\rho}_2 &= \rho + \mathbf{r}'. \end{aligned} \quad (\text{B7})$$

The integrals (B5), (B6) depend only on the relative distances $\boldsymbol{\rho}_1, \boldsymbol{\rho}_2$. Also, due to the boundary conditions, the path $\hat{\boldsymbol{\rho}}_s(\xi)$ turns out to be ξ -independent in (B5) and (B6).

Equation (B4) provides an explicit expression for the in-medium average of pairs of Green's functions as long as both Green's functions are for particles with the same momentum p . To calculate the radiation probability (2.17), we have to extend this calculation to the case of two different momenta. To this end, we use the identity

$$1 = \mathcal{N}(\mathbf{r}, \boldsymbol{\rho}) \int \mathcal{D}\mathbf{r}_e \exp \left\{ \frac{ip}{2} x \int_z^{z'} \dot{\mathbf{r}}_e^2(\xi) d\xi \right\}, \quad (\text{B8})$$

where the norm $\mathcal{N}(\mathbf{r}, \boldsymbol{\rho})$ is given in terms of the boundary conditions for the path integral over \mathbf{r}_e ,

$$\mathcal{N}(\mathbf{r}, \boldsymbol{\rho}) = \frac{2\pi i (z' - z)}{p x} \exp \left\{ -\frac{i p x}{2(z' - z)} (\mathbf{r} - \boldsymbol{\rho})^2 \right\}, \quad (\text{B9})$$

$$\mathbf{r}_e(z) \equiv \mathbf{r}(z) = \mathbf{r}, \quad \mathbf{r}_e(z') \equiv \mathbf{r}(z') = \boldsymbol{\rho}. \quad (\text{B10})$$

This allows us to write

$$\begin{aligned} & \langle G(z', \boldsymbol{\rho}; z, \mathbf{r} | p(1-x)) G^*(z', \mathbf{r}'; z, \boldsymbol{\rho}' | p) \rangle \\ &= \mathcal{N}(\mathbf{r}, \boldsymbol{\rho}) \int \mathcal{D}\mathbf{r} \mathcal{D}\mathbf{r}' \mathcal{D}\mathbf{r}_e \mathcal{F}(\mathbf{r} - \mathbf{r}') \\ & \times \exp \left\{ \frac{ip}{2} \int_z^{z'} [(1-x) \dot{\mathbf{r}}^2 + x \dot{\mathbf{r}}_e^2 - \dot{\mathbf{r}}'^2] d\xi \right\}, \quad (\text{B11}) \end{aligned}$$

where $\mathbf{r}'(z') = \mathbf{r}'$ and $\mathbf{r}'(z) = \boldsymbol{\rho}'$. Introducing the new coordinates

$$\mathbf{r}_a(\xi) = (1-x) \mathbf{r}(\xi) + x \mathbf{r}_e(\xi), \quad (\text{B12})$$

$$\mathbf{r}_b(\xi) = \mathbf{r}(\xi) - \mathbf{r}_e(\xi), \quad (\text{B13})$$

the exponent of the path integral (B10) reads

$$(1-x) \dot{\mathbf{r}}^2 + x \dot{\mathbf{r}}_e^2 - \dot{\mathbf{r}}'^2 = \dot{\mathbf{r}}_a^2 - \dot{\mathbf{r}}'^2 + (1-x)x \dot{\mathbf{r}}_b^2, \quad (\text{B14})$$

and \mathcal{F} appears with the argument $\mathcal{F}(\mathbf{r}_a - \mathbf{r}' + x \mathbf{r}_b)$. In complete analogy to the calculation of (B4), this renders the path integral over $(\mathbf{r}_a + \mathbf{r}')$ trivial and reduces the support of $(\mathbf{r}_a - \mathbf{r}')$ to a straight line. With the choice of boundary conditions (B9), we find

$$\begin{aligned} & \langle G(z', \boldsymbol{\rho}; z, \mathbf{r} | p_2) G^*(z', \mathbf{r}'; z, \boldsymbol{\rho}' | p_1) \rangle = \frac{-p}{2\pi i (z' - z)} \frac{1}{x} \\ & \times \exp \left\{ \frac{ip}{2(z' - z)} [(1-x)(\boldsymbol{\rho} - \mathbf{r})^2 - (\mathbf{r}' - \boldsymbol{\rho}')^2] \right\} \\ & \times \int \mathcal{D}\mathbf{r}_b \exp \left\{ \frac{i\mu}{2} \int_z^{z'} \dot{\mathbf{r}}_b^2 - \int_z^{z'} \Sigma(\xi, \hat{\boldsymbol{\rho}}_f + x \mathbf{r}_b) d\xi \right\}, \quad (\text{B15}) \end{aligned}$$

where $\mu = p(1-x)x$ and

$$\hat{\boldsymbol{\rho}}_f(\xi) = \boldsymbol{\rho}_2 \frac{\xi - z}{z' - z} + \boldsymbol{\rho}_1 \frac{z' - \xi}{z' - z}. \quad (\text{B16})$$

We can now simplify the radiation probability $\langle |M_{fi}|^2 \rangle$ of (2.18) with the help of (B5), (B6) and (B15). To this aim, we observe first that with a partial integration, the derivative $\partial/\partial \mathbf{r} \partial/\partial \mathbf{r}'$ of the interaction vertex (2.17) changes into $-\partial/\partial \boldsymbol{\rho}_1 \partial/\partial \boldsymbol{\rho}_2$. Then we change to the integration variables

$$\begin{aligned} \boldsymbol{\tau} &= \bar{\boldsymbol{\rho}}_1 - \bar{\boldsymbol{\rho}}_2, \quad \bar{\boldsymbol{\tau}} = \bar{\boldsymbol{\rho}}_1 + \bar{\boldsymbol{\rho}}_2, \\ \mathbf{b} &= \frac{1}{4} \bar{\boldsymbol{\tau}} = \frac{1}{4} (\mathbf{r} + \boldsymbol{\rho}' + \boldsymbol{\rho} + \mathbf{r}'). \end{aligned} \quad (\text{B17})$$

The only $\boldsymbol{\tau}$ -dependence of the integrand of $\langle |M_{fi}|^2 \rangle$ is in the exponential of the second line of (B15). Rewriting this in the new integration variables (B7) and (B17), we find

$$\begin{aligned} & \int d\boldsymbol{\tau} \exp \left\{ \frac{ip}{2(z' - z)} [(\boldsymbol{\rho}_1 - \boldsymbol{\rho}_2) \cdot \boldsymbol{\tau} - \frac{x}{4} ((\boldsymbol{\rho}_1 - \boldsymbol{\rho}_2) + \boldsymbol{\tau})^2] \right\} \\ &= \frac{-8\pi i (z' - z)}{p x} \exp \left\{ \frac{ip(1-x)}{2(z' - z)x} (\boldsymbol{\rho}_1 - \boldsymbol{\rho}_2)^2 \right\}. \quad (\text{B18}) \end{aligned}$$

The radiation probability reads now

$$\begin{aligned} \langle |M_{fi}|^2 \rangle &= \frac{8}{x^2} \text{Re} \int d\boldsymbol{\rho}_1 d\boldsymbol{\rho}_2 d\mathbf{b} \int dz \int_z^\infty dz' \\ & \times \exp \{ i\bar{q}(z' - z) + i\mathbf{p}_{1\perp} \cdot \boldsymbol{\rho}_1 - i\mathbf{p}_{2\perp} \cdot \boldsymbol{\rho}_2 \} \\ & \times \exp \left\{ -\int_{z-}^z \Sigma(\xi, \boldsymbol{\rho}_1) d\xi - \int_{z'}^{z+} \Sigma(\xi, \boldsymbol{\rho}_2) d\xi \right\} \\ & \times \hat{\Gamma}_{-\boldsymbol{\rho}_1} \hat{\Gamma}_{-\boldsymbol{\rho}_2}^* \exp \left\{ \frac{ip(1-x)}{2(z' - z)x} (\boldsymbol{\rho}_1 - \boldsymbol{\rho}_2)^2 \right\} \\ & \times \int \mathcal{D}\mathbf{r}_b \exp \left\{ \frac{ip(1-x)x}{2} \int_z^{z'} \dot{\mathbf{r}}_b^2(\xi) d\xi \right\} \\ & \times \exp \left\{ -\int_z^{z'} \Sigma(\xi, \hat{\boldsymbol{\rho}}_f + x \mathbf{r}_b) d\xi \right\}. \quad (\text{B19}) \end{aligned}$$

This is proportional to a transverse area $d\mathbf{b}$ which we devote out in what follows: the corresponding radiation spectrum is given per unit transverse area. The above expression can be simplified further if one observes that

$$\int_z^{z'} (\dot{\hat{\boldsymbol{\rho}}}_f + \dot{\mathbf{r}}_b)^2 d\xi = \frac{(\boldsymbol{\rho}_1 - \boldsymbol{\rho}_2)^2}{(z' - z)} + \int_z^{z'} \dot{\mathbf{r}}_b^2 d\xi. \quad (\text{B20})$$

After a transformation $\boldsymbol{\rho}_1 \rightarrow x \boldsymbol{\rho}_1$, and $\boldsymbol{\rho}_2 \rightarrow x \boldsymbol{\rho}_2$, this allows to combine in (B19) the Gaussian exponent and the path integral into a new path integral over

$$\mathbf{r}_c(\xi) = \hat{\boldsymbol{\rho}}_f(\xi) + \mathbf{r}_c(\xi), \quad (\text{B21})$$

with boundary conditions

$$\begin{aligned} \mathbf{r}_c(z) &= \hat{\boldsymbol{\rho}}_f(z) = \boldsymbol{\rho}_1, \\ \mathbf{r}_c(z') &= \hat{\boldsymbol{\rho}}_f(z') = \boldsymbol{\rho}_2. \end{aligned} \quad (\text{B22})$$

The resulting expression is given in (2.22) and differs from the result of Ref. [27] by the regularization $\exp\{-\epsilon|z|\}$ of the integrand only. The extension of the formalism to spin- and helicity dependent quantities is obtained, by inserting for $\hat{\Gamma}_{-\rho_1}$ and $\hat{\Gamma}_{-\rho_2}^*$ in (B19) the spin- and helicity dependent vertex functions (2.15) and (2.16), rather than the average (2.17).

APPENDIX C: MULTIPLE SCATTERINGS: N=3

For the case of $N = 3$ scatterings, the combined momentum transfer \mathbf{q}_\perp from the medium is described by the folding of three elastic Mott cross sections $\tilde{\Sigma}$,

$$\int d\mathcal{V}^3(\mathbf{q}_\perp) \equiv - \int d\mathbf{q}_{1\perp} d\mathbf{q}_{2\perp} d\mathbf{q}_{3\perp} \tilde{\Sigma}(\mathbf{q}_{1\perp}) \tilde{\Sigma}(\mathbf{q}_{2\perp}) \tilde{\Sigma}(\mathbf{q}_{3\perp}) \times \frac{(2\pi)^2}{x^2} \delta^{(2)}(\mathbf{q}_\perp - \mathbf{q}_{1\perp} - \mathbf{q}_{2\perp} - \mathbf{q}_{3\perp}). \quad (\text{C1})$$

With the shorthands

$$\begin{aligned} \mathbf{u}_{m1} &= x (\mathbf{p}_{1\perp} + \mathbf{q}_{1\perp}), \\ \mathbf{u}_{m2} &= x (\mathbf{p}_{1\perp} + \mathbf{q}_{1\perp} + \mathbf{q}_{2\perp}), \\ Q_{m1} &= \frac{\mathbf{u}_{m1}^2}{2\mu}, \quad Q_{m2} = \frac{\mathbf{u}_{m2}^2}{2\mu}, \end{aligned} \quad (\text{C2})$$

the radiation spectrum (2.22) expanded to third order reads

$$\begin{aligned} \frac{d^5\sigma}{d(\ln x) d\mathbf{p}_\perp d\mathbf{k}_\perp} \Big|_{O(\alpha_{\text{em}}^7 \mathcal{T}^3)} &= C_{\text{pre}} g_{\text{nf}} \int d\mathcal{V}^3(\mathbf{q}_\perp) \\ &\times \left[\frac{1}{3!} \mathbf{u}_2^2 \mathcal{Z}_1^{(3)} + \frac{1}{2} \mathbf{u}_{m2}^2 \mathcal{Z}_2^{(3)} + \frac{1}{2} \mathbf{u}_{m1}^2 \mathcal{Z}_3^{(3)} + \frac{1}{3!} \mathbf{u}_1^2 \mathcal{Z}_4^{(3)} \right. \\ &+ \frac{1}{2} \mathbf{u}_2 \cdot \mathbf{u}_{m2} \mathcal{Z}_5^{(3)} + \frac{1}{2} \mathbf{u}_1 \cdot \mathbf{u}_{m1} \mathcal{Z}_6^{(3)} \\ &+ \mathbf{u}_{m1} \cdot \mathbf{u}_{m2} \mathcal{Z}_7^{(3)} + \mathbf{u}_2 \cdot \mathbf{u}_{m1} \mathcal{Z}_8^{(3)} \\ &\left. + \mathbf{u}_{m2} \cdot \mathbf{u}_1 \mathcal{Z}_9^{(3)} + \mathbf{u}_1 \cdot \mathbf{u}_2 \mathcal{Z}_{10}^{(3)} \right] n_0^3. \end{aligned} \quad (\text{C3})$$

The variables $\mathcal{Z}_i^{(3)}$ stand again for the longitudinal integrals over phase factors. For a homogeneous medium of density n_0 and length L they read

$$\mathcal{Z}_1^{(3)} = \frac{L^3}{2Q_2^2}, \quad (\text{C4})$$

$$\mathcal{Z}_2^{(3)} = \frac{6 \sin(L Q_{m2}) - 6 L Q_{m2} + L^3 Q_{m2}^3}{3 Q_{m2}^5}, \quad (\text{C5})$$

$$\mathcal{Z}_3^{(3)} = \frac{6 \sin(L Q_{m1}) - 6 L Q_{m1} + L^3 Q_{m1}^3}{3 Q_{m1}^5}, \quad (\text{C6})$$

$$\mathcal{Z}_4^{(3)} = \frac{L^3}{2Q_1^2}, \quad (\text{C7})$$

$$\mathcal{Z}_5^{(3)} = -\frac{6 \sin(L Q_{m2}) - 6 L Q_{m2} + L^3 Q_{m2}^3}{3 Q_2 Q_{m2}^4}, \quad (\text{C8})$$

$$\mathcal{Z}_6^{(3)} = -\frac{6 \sin(L Q_{m1}) - 6 L Q_{m1} + L^3 Q_{m1}^3}{3 Q_1 Q_{m1}^4}, \quad (\text{C9})$$

$$\begin{aligned} \mathcal{Z}_7^{(3)} &= -\frac{L^3}{6 Q_1 Q_2} + \frac{(\sin(L Q_{m1}) - L Q_{m1})}{Q_{m1}^4 (Q_{m1} - Q_{m2})} \\ &\quad - \frac{(\sin(L Q_{m2}) - L Q_{m2})}{(Q_{m1} - Q_{m2}) Q_{m2}^4}, \end{aligned} \quad (\text{C10})$$

$$\begin{aligned} \mathcal{Z}_8^{(3)} &= \frac{(\sin(L Q_{m2}) - L Q_{m2})}{Q_2 (Q_{m1} - Q_{m2}) Q_{m2}^3} \\ &\quad - \frac{(\sin(L Q_{m1}) - L Q_{m1})}{Q_2 Q_{m1}^3 (Q_{m1} - Q_{m2})}, \end{aligned} \quad (\text{C11})$$

$$\begin{aligned} \mathcal{Z}_9^{(3)} &= \frac{(\sin(L Q_{m2}) - L Q_{m2})}{Q_1 (Q_{m1} - Q_{m2}) Q_{m2}^3} \\ &\quad - \frac{(\sin(L Q_{m1}) - L Q_{m1})}{Q_1 Q_{m1}^3 (Q_{m1} - Q_{m2})}, \end{aligned} \quad (\text{C12})$$

$$\begin{aligned} \mathcal{Z}_{10}^{(3)} &= \frac{(\sin(L Q_{m1}) - L Q_{m1})}{Q_1 Q_2 Q_{m1}^2 (Q_{m1} - Q_{m2})} \\ &\quad - \frac{(\sin(L Q_{m2}) - L Q_{m2})}{Q_1 Q_2 (Q_{m1} - Q_{m2}) Q_{m2}^2}. \end{aligned} \quad (\text{C13})$$

From this one finds again the simple limiting cases. We confirm the factorization limit

$$\begin{aligned} \lim_{L \rightarrow 0} \frac{d^5\sigma}{d(\ln x) d\mathbf{p}_\perp d\mathbf{k}_\perp} \Big|_{O(\alpha_{\text{em}}^7 \mathcal{T}^3)}^{\mathcal{T} \text{ fixed}} &= C_{\text{pre}} g_{\text{nf}} \frac{\mathcal{T}^3}{12} \left(\frac{\mathbf{u}_1}{Q_1} - \frac{\mathbf{u}_2}{Q_2} \right)^2 \int d\mathcal{V}^3(\mathbf{q}_\perp), \end{aligned} \quad (\text{C14})$$

and the Bethe-Heitler limit

$$\begin{aligned} \lim_{L \rightarrow \infty} \frac{d^5\sigma}{d(\ln x) d\mathbf{p}_\perp d\mathbf{k}_\perp} \Big|_{O(\alpha_{\text{em}}^7 \mathcal{T}^3)}^{\mathcal{T} \text{ fixed}} &= C_{\text{pre}} g_{\text{nf}} \int d\mathcal{V}^3(\mathbf{q}_\perp) \\ &\times \frac{\mathcal{T}^3}{12} \left[\left(\frac{\mathbf{u}_1}{Q_1} - \frac{\mathbf{u}_{m1}}{Q_{m1}} \right)^2 + \left(\frac{\mathbf{u}_{m1}}{Q_{m1}} - \frac{\mathbf{u}_{m2}}{Q_{m2}} \right)^2 \right. \\ &\left. + \left(\frac{\mathbf{u}_{m2}}{Q_{m2}} - \frac{\mathbf{u}_2}{Q_2} \right)^2 \right]. \end{aligned} \quad (\text{C15})$$

Also, we have checked in complete analogy to the case of $N = 2$ scatterings that the lowest order correction to the factorization limit (C14) is proportional to L^2 times \mathcal{T}^3 . The \mathbf{q}_\perp -integral of this correction diverges logarithmically. This further corroborates the conclusions drawn in subsection III B.

-
- [1] L.D. Landau and I.Ya. Pomeranchuk, Dokl. Akad. Nauk. SSSR **92** (1953) 535, 735.
 - [2] V.B. Berestetski, E.M. Lifshits and L.P. Pitaevski, *Landau Course of Theoretical Physics Vol. IV*, Oxford, Pergamon Press, 1979.

- [3] A.B. Migdal, Phys. Rev. **103** (1956) 1811.
- [4] J.S. Bell, Nucl. Phys. **8** (1958) 613.
- [5] S. Klein, hep-ph/9802442, submitted to *Review of Modern Physics*.
- [6] M.L. Ter-Mikaelian, JETP **25** (1953) 289.
- [7] SLAC-146 Coll., P. Anthony et al., Phys. Rev. Lett. **75** (1995) 1949.
- [8] SLAC-146 Coll., P. Anthony et al., Phys. Rev. **D 56** (1997) 1373.
- [9] SLAC-146 Coll., P. Anthony et al., Phys. Rev. Lett. **76** (1996) 3550.
- [10] R. Blankenbecler and S.D. Drell, Phys. Rev. **D 53** (1996) 6265.
- [11] R. Blankenbecler, Phys. Rev. **D55** 190.
- [12] V.N. Baier and V.M. Katkov, Phys. Rev. **D57** (1998) 3146;
- [13] V.N. Baier and V.M. Katkov, Phys. Rev. **D59** (1999) 056003.
- [14] V.N. Baier and V.M. Katkov, hep-ph/9902436.
- [15] B.G. Zakharov, JETP Letters **63** (1996) 952, **65** (1997) 615.
- [16] B.G. Zakharov, hep-ph/9805271.
- [17] B.G. Zakharov, Phys. Atom. Nucl. **61** (1998) 838 [Yad. Fiz. **61** (1998) 924], hep-ph/9807540.
- [18] R. Baier, Y.L. Dokshitzer, A.H. Mueller, S. Peigné and D. Schiff, Nucl. Phys. **B478** (1996) 577.
- [19] I.M. Dremin and C.S. Lam, Mod. Phys. Lett. **A13** (1998) 2789.
- [20] J. Knoll and D.N. Voskresensky, Annals Phys. **249** (1996) 532; Phys. Lett. **B351** (1995) 43.
- [21] M. Gyulassy and X.-N. Wang, Nucl. Phys. **B420** (1994) 583.
- [22] X.-N. Wang, M. Gyulassy and M. Plümer, Phys. Rev. **D51** (1995) 3436.
- [23] R. Baier, Y.L. Dokshitzer, A.H. Mueller, S. Peigné and D. Schiff, Nucl. Phys. **B483** (1997) 291.
- [24] R. Baier, Y.L. Dokshitzer, A.H. Mueller, S. Peigné and D. Schiff, Nucl. Phys. **B484** (1997) 265.
- [25] R. Baier, Y.L. Dokshitzer, A.H. Mueller and D. Schiff, Phys. Rev. **C58** (1998) 1706.
- [26] R. Baier, Y.L. Dokshitzer, A.H. Mueller and D. Schiff, Nucl. Phys. **B531** (1998) 403.
- [27] B.Z. Kopeliovich, A. Schäfer and A.V. Tarasov, Phys. Rev. **C59** (1999) 1609.
- [28] B.Z. Kopeliovich, J. Raufeisen and A.V. Tarasov, Phys. Lett. **B440** (1998) 151.
- [29] J. Raufeisen, A.V. Tarasov and O.O. Voskresenskaya, hep-ph/9812398, Eur. Phys. J. C in press.
- [30] N.N. Nikolaev and B.G. Zakharov, JETP **78** (1994) 598.
- [31] C. Itzykson and J.-B. Zuber, *Quantum Field Theory*, New York, McGraw-Hill, 1985.
- [32] B.G. Zakharov, Sov. J. Nucl. Phys. **46** (1987) 92.
- [33] S.J. Brodsky, A. Hebecker, and E. Quack, Phys. Rev. **D55** (1997) 2584.
- [34] M. Gyulassy, P. Levai and I. Vitev, hep-ph/9907461.
- [35] Y.-S. Tsai, Rev. Mod. Phys. **46** (1974) 815.
- [36] J.F. Gunion and G. Bertsch, Phys. Rev. **D25** (1982) 746.